

Supplementary information

Half sandwich Ru(II)-acylthioureas complexes: DNA/HSA-binding, anti-migration and cell death properties in a breast tumor cell line

Legna Colina-Vegas^{a*}, Liany Luna-Dulcey^b, Ana M. Plutín^c, Eduardo E. Castellano^d, Marcia R. Cominetti^b, Alzir Azevedo Batista^{a*}

TABLE OF CONTENTS

Scheme 1S. Numbering data for NMR identification of acylthiourea ligands

Figure 1S. UV-Vis spectrum of metal complexes in dichloromethane solutions at room temperature

Figure 2S-9S. The 2D heteronuclear ^1H - ^{13}C HMBC NMR spectra of ligands and $\text{Ru}(\eta^6\text{-}p\text{-cymene})(\text{L}_n)(\text{Cl})_2$ (**1-6**) or $\text{Ru}(\eta^6\text{-}p\text{-cymene})(\text{L}_n)\text{Cl}$ (**7-8**) in DMSO-d_6 at 300 K

Figure 10S. Cyclic voltammogram for complexes in CH_2Cl_2 , (Tetrabutylammonium perchlorate 0.1 M; Ag/AgCl; work electrode Pt; 100 mV.s $^{-1}$)

Figure 11S. ESI-MS spectrum of complexes in acetone

Table 1S. Crystal data and structure refinement for metal complexes **1**, **2**, **3** and **6**

Figure 12S. ORTEP view of complexes **1**, **2**, **3** and **6** with the thermal ellipsoids at the 50 % probability level. The hydrogens have been omitted for clarity

Table 2S. IC_{50} values in 24 h against A549 tumor cell line by MTT assay

Figure 13S. MDA-MB-231 morphology in different concentrations of Ru-acylthiourea complexes

Figure 14S. MDA-MB-231 colony inhibition

Figure 15S. Wound healing assay

Figure 16S. MDA-MB-231 migration in Boyden chamber assay for complexes (**6**) and (**8**).

Figure 17S. (A) Spectrophotometric titration spectra of complex **8** calf thymus (CT) DNA. [DNA] = 0– 1.78×10^{-4} M. (B) Circular dichroism (CD) spectra of CT DNA incubated 18 h with the complex **8** at different [complex]/[DNA] ratios at 37 °C

Figure 18S. Spectrophotometric titration spectra of compounds with CT-DNA

Figure 19S. Circular dichroism (CD) spectra of CT-DNA incubated 18 h with the complexes at 37 °C

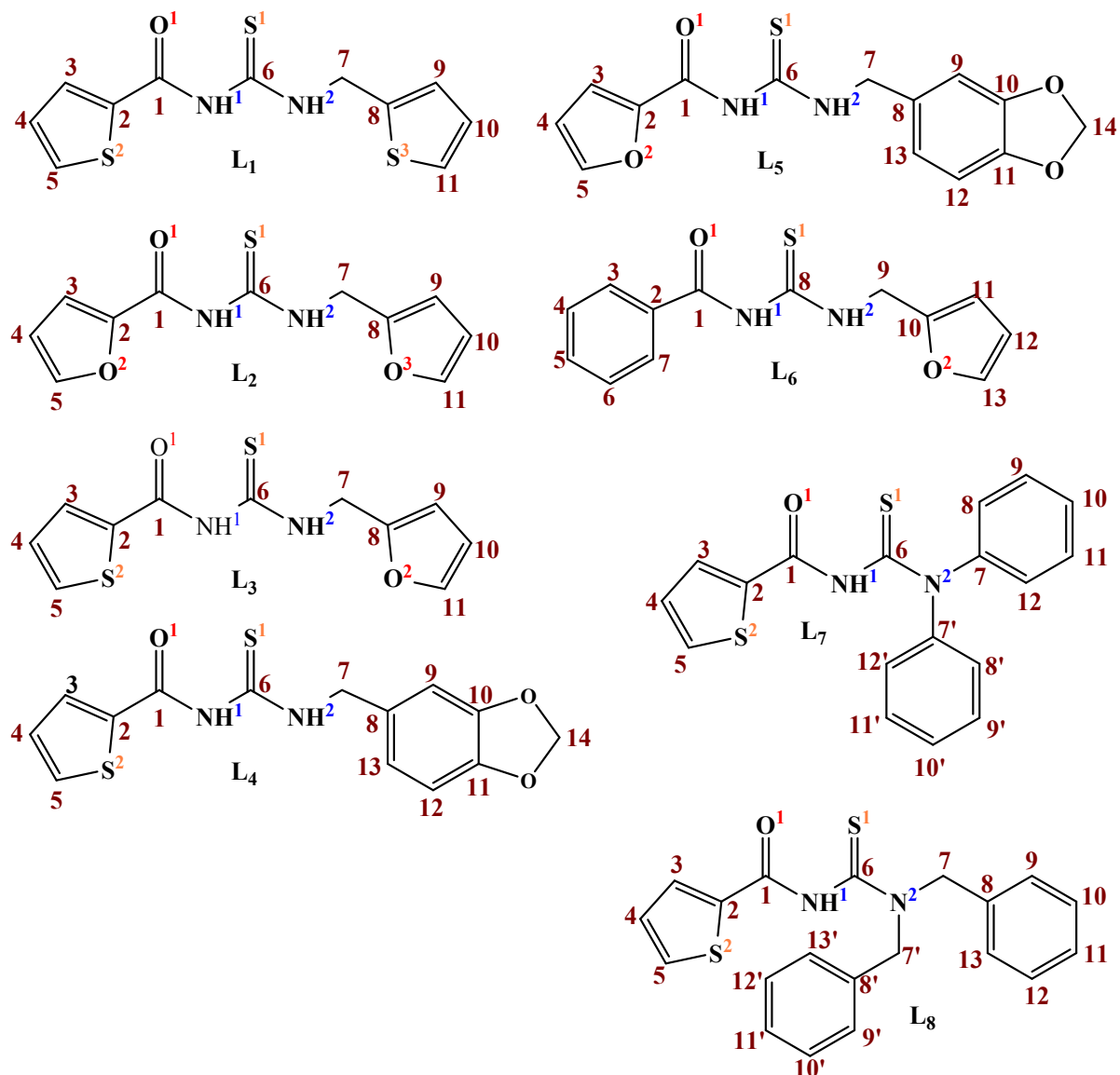
Figure 20S. Effects of the concentration of complexes **5-8** on the fluorescence of DNA-thiazole orange (TO) adduct

Figure 21S. Effects of the concentration of complexes **1**, **2**, **5-8** on the electrophoresis of plasmid pBR322 DNA. Molecular weight marker (1) and DNA in DMSO (2). Ri 0.5, 1.0, 2.0 and 4.0 of metal complex **1** (3-6), **2** (7-10), **5** (11-14), **6** (15-18), **7** (19-22), **8** (23-26)

Figure 22S. ^1H NMR in dmso-d_6 of a mixture of complex **5** and guanosine

Figure 23S. Fluorescence quenching spectra of HSA with different concentrations of Ru(II)-acylthiourea complexes at 310 K. The arrow shows the intensity changes upon increasing the concentration of the quencher

Figure 24S. Stern–Volmer plots showing tryptophan quenching in HSA at 310 K



Scheme 1S. Numbering data for NMR identification of acylthiourea ligands

N-(2-thiophenecarbonyl)-N'-(2-thiophenemethyl)thiourea (L_1). Brown solid. Molecular weight (MW): 262. Elemental analysis for $\text{C}_{11}\text{H}_{10}\text{N}_2\text{OS}_3$: found (calculated) C 47.00 (46.78), H 3.60 (3.57), N 9.98 (9.92), S 33.99 (34.06). FT-IR (cm^{-1}): ($\nu\text{N-H}$) 3194; ($\nu\text{C-H}$) 3057, 2939; ($\nu\text{C=O}$) 1665; ($\nu\text{C=C}$) 1547; ($\nu\text{C=S}$) 1276; ($\gamma\text{C=S}$) 750. NMR ^1H 400 MHz, dmso-d₆ (multiplicity, attribution, coupling constant): δ 11.50 (s, NH¹), 11.06 (t, NH², $J^3 = 5.6$ Hz), 8.33 (dd, H5, $J^3 = 4.0$ Hz, $J^4 = 0.8$ Hz), 8.00 (dd, H3, $J^3 = 4.9$ Hz, $J^4 = 0.8$ Hz), 7.44 (dd, H11, $J^3 = 5.0$ Hz, $J^4 = 1.2$ Hz), 7.21 (dd, H4, $J^3 = 4.9$ Hz, 4.0 Hz), 7.13 (d, H9, $J^3 = 3.2$ Hz), 6.99 (dd, H10, $J^3 = 5.0$ Hz, 3.2 Hz), 5.02 (d, H7, $J^3 = 5.6$ Hz). NMR $^{13}\text{C}\{\text{H}\}$ dmso-d₆ (assignment, δ): C6 179.83, C1 161.85, C8 139.42, C2 136.69, C3 135.08, C5, 132.46, C4 128.67, C9 126.97, C10 126.62, C11 125.78, C7 42.92.

N-(2-furoyl)-N'-(2-furfuryl)thiourea (L_2). Light brown solid. MW: 250.04. Elemental analysis for $\text{C}_{11}\text{H}_{10}\text{N}_2\text{O}_3\text{S}$: C 52.90 (52.79), H, 4.10 (4.03), N 10.90 (11.19), S 12.92 (12.81). FT-IR (cm^{-1}): ($\nu\text{N-H}$) 3251; ($\nu\text{C-H}$) 3047, 2946; ($\nu\text{C=O}$) 1665; ($\nu\text{C=C}$) 1584; ($\nu\text{C=S}$) 1254; ($\gamma\text{C=S}$) 757. NMR ^1H 400 MHz, dmso-d₆: δ 11.20 (s, NH¹), 10.92 (t, NH², $J^3 = 5.2$ Hz), 8.03 (s, H5), 7.80 (d, H3, $J^3 = 3.3$ Hz), 7.63 (s, H11), 6.72 (dd, H4, $J^3 = 3.3$ Hz, 1.6 Hz), 6.43 (d, H9, $J^3 = 2.0$ Hz), 6.39 (d, H10, $J^3 = 2.0$ Hz), 4.85 (d, H7, $J^3 = 5.2$ Hz). NMR $^{13}\text{C}\{\text{H}\}$ dmso-d₆ (assignment, δ): C6 180.11, C1 157.60, C8 149.94, C5 148.28, C2 144.58, C11 142.69, C3 118.42, C4 112.56, C9 110.57, C10 108.12, C7 41.48.

N-(2-thiophenecarbonyl)-N'-(2-furfuryl)thiourea (L_3). Orange solid. MW: 266.02. Elemental analysis for $\text{C}_{11}\text{H}_{10}\text{N}_2\text{O}_2\text{S}_2$: C 49.69 (49.61), H, 3.86 (3.78), N, 10.76 (10.52), S 23.86 (24.08). UV-Vis. FT-IR (cm^{-1}): ($\nu\text{N-H}$) 3189; ($\nu\text{C-H}$) 3064, 2933; ($\nu\text{C=O}$) 1650; ($\nu\text{C=C}$) 1553; ($\nu\text{C=S}$) 1279; ($\gamma\text{C=S}$) 745. NMR ^1H 400 MHz, dmso-d₆: δ 11.54 (s, NH¹), 11.02 (t, NH², $J^3 = 5.1$ Hz), 8.35 (dd, H5, $J^3 = 3.9$, $J^4 = 1.1$ Hz), 8.01 (dd, H3, $J^3 = 5.0$, $J^4 = 1.0$ Hz), 7.64 (dd, H11, $J^3 = 1.8$, $J^4 = 0.8$ Hz), 7.22 (dd, H4, $J^3 = 5.0$, 3.9 Hz), 6.42 (dd, H9, $J^3 = 4.0$, $J^4 = 0.8$ Hz), 4.85 (dd, H10, $J^3 = 4.0$, 1.8 Hz), 3.34 (s, H7). NMR $^{13}\text{C}\{\text{H}\}$ dmso-d₆ (assignment, δ): C6 180.164, C1 162.075, C8 149.918, C11 142.72, C2 136.64, C3 135.13, C5 132.53, C4 128.67, C9 110.58, C10 108.14, C7 41.49.

N-(2-thiophenecarbonyl)-N'-piperonylthiourea (L_4). Light brown solid. MW: 320.03. Elemental analysis for $\text{C}_{14}\text{H}_{12}\text{N}_2\text{O}_3\text{S}_2$: C 52.34 (52.48), H 3.75 (3.78), N 8.51 (8.74), S 20.20 (20.02). FT-IR (cm^{-1}): ($\nu\text{N-H}$) 3216; ($\nu\text{C-H}$) 3073, 2933; ($\nu\text{C=O}$) 1656; ($\nu\text{C=C}$) 1553; ($\nu\text{C=S}$) 1260; ($\gamma\text{C=S}$) 732. NMR ^1H 400 MHz, dmso-d₆: δ 11.45 (s, NH¹), 11.00 (t, NH², $J^3 = 5.5$ Hz), 8.33 (dd, H5, $J^3 = 4.0$ Hz, $J^4 = 0.9$ Hz), 8.00 (dd, H3, $J^3 = 5.0$ Hz, $J^4 = 0.9$ Hz), 7.22 (dd, H4, $J^3 = 5.0$, 4.0 Hz), 6.98 (s, H9), 6.87 (m, H10, H13), 6.00 (s, H14), 4.73 (d, H7, $J^3 = 5.5$ Hz). NMR $^{13}\text{C}\{\text{H}\}$ dmso-d₆ (assignment, δ): C6 179.88, C1 161.89, C12 147.29, C11 146.48, C2 136.78, C3 135.00, C5 132.39, C8 130.96, C4 128.66, C9 121.18, C10 108.35, C13 108.18, C14 100.94, C7 47.95.

N-(2-furoyl)-N'-piperonylthiourea (L_5). Beige solid. MW: 300.05. Elemental analysis for $\text{C}_{14}\text{H}_{12}\text{N}_2\text{O}_4\text{S}$: C 55.08 (55.25), H 4.15 (3.97), N 9.57 (9.21), S 10.26 (10.54). FT-IR (cm^{-1}): ($\nu\text{N-H}$) 3260; ($\nu\text{C-H}$) 3047, 2943; ($\nu\text{C=O}$) 1663; ($\nu\text{C=C}$) 1585; ($\nu\text{C=S}$) 1261; ($\gamma\text{C=S}$) 749. NMR ^1H 400 MHz, dmso-d₆: δ 11.09 (s, NH¹), 10.92 (t, NH², $J^3 = 5.6$ Hz), 8.03 (m, H5), 7.80 (d, H3, $J^3 = 3.5$ Hz, $J^4 = 0.6$ Hz), 6.98 (s, H9), 6.87 (m, H10, H13), 6.72 (m, H4), 6.00 (s, H14), 4.74 (d, H7, $J^3 = 5.6$ Hz). NMR $^{13}\text{C}\{\text{H}\}$ dmso-d₆ (assignment, δ): C6 179.84, C1 157.44, C5 148.17, C12 147.29, C11 146.47, C2 144.68, C8 131.00, C9 121.14, C3 118.25, C4 112.53, C10 108.32, C9 108.15, C14 100.93, C7 47.93.

N-benzoyl-N'-(2-furfuryl)thiourea (L_6). Brown solid. MW: 260.06. Elemental analysis for $\text{C}_{13}\text{H}_{12}\text{N}_2\text{O}_2\text{S}$: C 60.00 (59.98), H 4.95 (4.65), N 10.99 (10.76), S 12.60 (12.32). FT-IR (cm^{-1}): ($\nu\text{N-H}$) 3228; ($\nu\text{C-H}$) 3048, 2962; ($\nu\text{C=O}$) 1665; ($\nu\text{C=C}$) 1549; ($\nu\text{C=S}$) 1261; ($\gamma\text{C=S}$) 744. NMR ^1H 400 MHz, dmso-d₆: δ 11.47 (s, NH¹), 11.16 (t, NH², $J^3 = 5.0$ Hz), 7.91 (m, H7 and H3), 7.63 (m, H5 and H13), 7.50 (m, H6 and H4), 6.43 (m, H11 and H12), 4.86 (d, H9, $J^3 = 5.6$ Hz). NMR $^{13}\text{C}\{\text{H}\}$ dmso-d₆ (assignment, δ): C6 180.51, C1 168.28, C10 149.96, C13 142.77, C5 133.04, C2 132.12, C4, C6 128.58, C3, C7 128.41, C11 110.63, C12 108.25, C9 41.465.

Ru(η^6 -*p*-cymene)(L_1)(Cl)₂ (1**).** Orange solid, yield 88 %. MW: 587.94. Elemental analysis for $\text{C}_{21}\text{H}_{24}\text{Cl}_2\text{N}_2\text{OS}_3\text{Ru}$: found (calculated) C 42.74 (42.85), H 3.95 (4.11), N 4.84 (4.76), S 16.22 (16.34). UV-Vis (CH_2Cl_2): λ nm (ϵ , $\text{M}^{-1}\text{cm}^{-1}$) 254 (8220), 294 (7580), 348 (2965), 440 (670). FT-IR (KBr, cm^{-1}): ($\nu\text{N-H}$) 3149; ($\nu\text{C-H}$) 3030, 2953; ($\nu\text{C=O}$) 1654; ($\nu\text{C=C}$) 1561; ($\nu\text{C=S}$) 1276; ($\gamma\text{C=S}$) 712; ($\nu\text{Ru-Cl}$) 284. NMR ^1H 400 MHz, dmso-d₆: δ 11.49 (s, 1H, NH¹), 11.06 (s, 1H, NH²), 8.33 (s, 1H, H5), 8.00 (d, 1H, H3, $J^3 = 4.3$ Hz), 7.44 (d, 1H, H11, $J^3 = 4.5$ Hz), 7.22 (s, 1H, H4), 7.13 (s, 1H, H9), 6.99 (s, 1H, H10), 5.81 (d, 2H, Ar-*p*-cym, $J^3 = 5.2$ Hz), 5.77 (d, 2H, Ar-*p*-cym, $J^3 = 5.2$ Hz) 5.03 (d, 2H, H7, $J^3 = 4.9$ Hz), 2.80 (hept, 1H, $\text{CH}(\text{CH}_3)_2$), 2.08 (s, 3H, CH₃), 1.19 (d, 6H, $\text{CH}(\text{CH}_3)_2$, $J^3 = 6.4$ Hz). NMR $^{13}\text{C}\{\text{H}\}$ dmso-d₆ (assignment, δ): C6 179.83, C1 161.84, C2 139.42, C8 136.69, C3 135.08, C5 132.47, C4 128.67, C9 126.96, C10 126.62, C11 125.78, CH-C 106.37, CH₃-C 100.07, Ar-*p*-cym 86.34, Ar-*p*-cym 85.48, C7 42.92, CH-(CH₃)₂ 29.96, CH-(CH₃)₂ 21.49, CH₃ 17.86. High resolution ESI(+)MS (acetone): 516.9506 [M-2Cl-H⁺]⁺.

Ru(η^6 -*p*-cymene)(L₂)(Cl)₂ (2). Light orange solid, yield 85 %. MW: 555.99. Elemental analysis for C₂₁H₂₄Cl₂N₂O₃SRu: C 45.21 (45.33), H 4.50 (4.35), N 5.21 (5.03), S 5.93 (5.71). UV-Vis (CH₂Cl₂): λ nm (ϵ , M⁻¹cm⁻¹) 254 (5700), 280 (7065), 338 (1990), 440 (430). FT-IR (KBr, cm⁻¹): (vN-H) 3233; (vC-H) 3029, 2959; (vC=O) 1677; (vC=C) 1568; (vC=S) 1254; (vC=S) 754; (vRu-Cl) 274. NMR ¹H 400 MHz, dmso-d₆: δ 11.18 (s, 1H, NH¹), 10.91 (s, 1H, NH²), 8.02 (s, 1H, H₅), 8.79 (d, 1H, H₃, J^3 = 4.0 Hz), 7.63 (s, 1H, H₁₁), 6.72 (s, 1H, H₄), 6.42 (m, 2H, H₉ and H₁₀), 5.80 (d, 2H, Ar-*p*-cym, J^3 = 6.0 Hz), 5.76 (d, 2H, Ar-*p*-cym, J^3 = 6.0 Hz), 4.84 (d, 2H, H₇, J^3 = 5.2 Hz), 2.82 (hept, 1H, CH(CH₃)₂), 2.08 (s, 3H, CH₃), 1.18 (d, 6H, CH(CH₃)₂, J^3 = 6.4 Hz). NMR ¹³C{¹H} dmso-d₆ (assignment, δ): C6 180.10, C1 157.59, C8 149.94, C5 148.28, C2 142.69, C11 118.42, C3 112.57, C4 110.58, C9 108.12, C10 106.38, CH-C 100.07, CH₃-C 86.34, Ar-*p*-cym 85.48, C7 41.49, CH-(CH₃)₂ 29.96, CH-(CH₃)₂ 21.48, CH₃ 17.85. High resolution ESI(+)-MS (acetone): 485.0059 [M-2Cl-H⁺]⁺.

Ru(η^6 -*p*-cymene)(L₃)(Cl)₂ (3). Orange solid, yield 87 %. MW: 571.97. Elemental analysis for C₂₁H₂₄Cl₂N₂O₂S₂Ru: C 44.28 (44.05), H 4.54 (4.23), N 5.02 (4.89), S 10.91 (11.20). UV-Vis (CH₂Cl₂): λ nm (ϵ , M⁻¹cm⁻¹) 256 (7920), 294 (5660), 342 (2360), 440 (540). FT-IR (KBr, cm⁻¹): (vN-H) 3212; (vC-H) 2958; (vC=O) 1650; (vC=C) 1569; (vC=S) 1286; (vC=S) 755; (vRu-Cl) 284. NMR ¹H 400 MHz, dmso-d₆: δ 11.53 (s, 1H, NH¹), 11.01 (s, 1H, NH²), 8.33 (d, 1H, H₅, J^3 = 3.0 Hz), 8.01 (d, 1H, H₃, J^3 = 4.4 Hz), 7.63 (s, 1H, H₁₁), 7.22 (m, 1H, H₄), 6.42 (m, 2H, H₉ and H₁₀), 5.81 (d, 2H, Ar-*p*-cym, J^3 = 6.0 Hz), 5.76 (d, 2H, Ar-*p*-cym, J^3 = 6.0 Hz), 4.84 (d, 2H, H₇, J = 5.4 Hz), 2.82 (hept, 1H, CH(CH₃)₂), 2.08 (s, 3H, CH₃), 1.18 (d, 6H, CH(CH₃)₂, J^3 = 6.6 Hz). NMR ¹³C{¹H} dmso-d₆ (assignment, δ): C6 180.16, C1 162.07, C8 149.91, C11 142.72, C2 136.63, C5 135.15, C3 132.53, C4 128.68, C9 110.59, C10 108.15, CH-C 106.38, CH₃-C 100.07, Ar-*p*-cym 86.34, Ar-*p*-cym 85.49, C7 41.49, CH-(CH₃)₂ 29.96, CH-(CH₃)₂ 21.48, CH₃ 17.85. High resolution ESI(+)-MS (acetone): 500.9829 [M-2Cl-H⁺]⁺.

Ru(η^6 -*p*-cymene)(L₄)(Cl)₂ (4). Orange solid, yield 92 %. MW: 625.98. Elemental analysis for C₂₄H₂₆Cl₂N₂O₃S₂Ru: C 46.36 (46.00), H 4.34 (4.18), N 4.73 (4.47), S 9.94 (10.23). UV-Vis (CH₂Cl₂): λ nm (ϵ , M⁻¹cm⁻¹) 256 (7870), 290 (7060), 342 (2240), 440 (515). FT-IR (KBr, cm⁻¹): (vN-H) 3205; (vC-H) 3063, 2957; (vC=O) 1662; (vC=C) 1566; (vC=S) 1263; (vC=S) 745; (vRu-Cl) 291. NMR ¹H 400 MHz, dmso-d₆: δ 11.44 (s, 1H, NH¹), 10.99 (s, 1H, NH²), 8.32 (d, 1H, H₅, J = 2.3 Hz), 7.99 (d, 1H, H₃, J^3 = 3.9 Hz), 7.21 (m, 1H, H₄), 6.97-6.87 (m, 3H, H₉, H₁₀ and H₁₃), 5.99 (s, 2H, H₁₄), 5.80 (d, 2H, Ar-*p*-cym, J^3 = 5.8 Hz), 5.76 (d, 2H, Ar-*p*-cym, J^3 = 5.8 Hz), 4.74 (d, 2H, H₇, J^3 = 5.2 Hz), 2.82 (hept, 1H, CH(CH₃)₂), 2.08 (s, 3H, CH₃), 1.18 (d, 6H, CH(CH₃)₂, J^3 = 6.6 Hz). NMR ¹³C{¹H} dmso-d₆ (assignment, δ): C6 179.89, C1 161.89, C12 147.30, C11 146.49, C2 136.78, C3 135.11, C5 132.54, C5 132.40, C8 130.96, C4 128.66, C9 121.19, C10 108.36, C13 108.18, CH-C 106.38, C14 100.94, CH₃-C 100.07, Ar-*p*-cym 85.61, Ar-*p*-cym 85.48, C7 47.96, CH-(CH₃)₂ 29.96, CH-(CH₃)₂ 21.48, CH₃ 17.85. High resolution ESI(+)-MS (acetone): 554.9948 [M-2Cl-H⁺]⁺.

Ru(η^6 -*p*-cymene)(L₅)(Cl)₂ (5). Yellow solid, yield 87 %. MW: 610.00. Elemental analysis for C₂₄H₂₆Cl₂N₂O₄SRu: C 47.52 (47.22), H 4.05 (4.29), 4.78 (4.59), S 4.97 (5.25). UV-Vis (CH₂Cl₂): λ nm (ϵ , M⁻¹cm⁻¹) 250 (6050), 284 (8290), 334 (2030), 440 (440). FT-IR (KBr, cm⁻¹): (vN-H) 3229; (vC-H) 3053, 2966; (vC=O) 1680; (vC=C) 1567; (vC=S) 1261; (vC=S) 758; (vRu-Cl) 267. NMR ¹H 400 MHz, dmso-d₆: δ 11.09 (s, 1H, NH¹), 10.91 (s, 1H, NH²), 8.02 (s, 1H, H₅), 7.78 (d, 1H, H₃, J^3 = 3.2 Hz), 6.97 (s, 1H, H₄), 6.87 (m, 2H, H₁₀ and H₁₃), 6.72 (m, 1H, H₉), 5.99 (s, 2H, H₁₄), 5.81 (d, 2H, Ar-*p*-cym, J^3 = 6.0 Hz), 5.76 (d, 2H, Ar-*p*-cym, J^3 = 6.0 Hz), 4.73 (d, 2H, H₇, J^3 = 5.6 Hz), 2.82 (hept, 1H, CH(CH₃)₂), 2.08 (s, 3H, CH₃), 1.18 (d, 6H, CH(CH₃)₂, J^3 = 6.6 Hz). NMR ¹³C{¹H} dmso-d₆ (assignment, δ): C6 179.84, C1 157.44, C5 148.19, C12 147.29, C11 146.47, C2 144.67, C8 130.99, C9 121.14, C3 118.26, C4 112.54, C10 108.16, CH-C 106.35, C14 100.94, CH₃-C 100.05, Ar-*p*-cym 86.35, Ar-*p*-cym 85.48, C7 47.92, CH-(CH₃)₂ 29.96, CH-(CH₃)₂ 21.48, CH₃ 17.86. High resolution ESI(+)-MS (acetone): 539.0087 [M-2Cl-H⁺]⁺.

Ru(η^6 -*p*-cymene)(L₆)(Cl)₂ (6). Orange solid, yield 94 %. MW: 566.01. Elemental analysis for C₂₃H₂₆Cl₂N₂O₃SRu: C 48.45 (48.76), H 4.38 (4.63), N 4.78 (4.94), 5.83 (5.66). UV-Vis (CH₂Cl₂): λ nm (ϵ , M⁻¹cm⁻¹) 254 (11560), 332 (2500), 440 (620). FT-IR (KBr, cm⁻¹): (vN-H) 3144; (vC-H) 3034, 2956; (vC=O) 1673; (vC=C) 1560; (vC=S) 1264; (vC=S) 749; (vRu-Cl) 282. NMR ¹H 400 MHz, dmso-d₆: δ 11.47 (s, 1H, NH¹), 11.15 (t, 1H, NH², J^3 = 5.0 Hz), 7.91 (m, 2H, H₇ and H₃), 7.63 (m, 2H, H₅ and H₁₃), 7.50 (m, 2H, H₆ and H₄), 6.43 (m, 2H, H₁₁ and H₁₂), 5.82 (d, 2H, Ar-*p*-cym, J^3 = 6.4 Hz), 5.77 (d, 2H, Ar-*p*-cym, J^3 = 6.4 Hz), 4.86 (d, 2H, H₉, J^3 = 5.2 Hz), 2.83 (hept, 1H, CH(CH₃)₂), 2.08 (s, 3H, CH₃), 1.18 (d, 6H, CH(CH₃)₂, J^3 = 6.6 Hz). NMR ¹³C{¹H} dmso-d₆ (assignment, δ): C6 180.47, C1 168.23, C10 149.93, C13 142.74, C5 133.00, C2 132.09, C3 14.6, 7.128.55, C11 110.59, C12 108.21, CH-C 106.35, CH₃-C 100.05, Ar-*p*-cym 86.34, Ar-*p*-cym 85.48, C9 41.43, CH-(CH₃)₂ 29.95, CH-(CH₃)₂ 21.48, CH₃ 17.85. High resolution ESI(+)-MS (acetone): 495.9174 [M-2Cl-H⁺]⁺.

Ru(η^6 -*p*-cymene)(L₇)Cl (7). Brown solid, yield 83 %. MW: 608.03. Elemental analysis for C₂₈H₂₇CIN₂OS₂Ru: C 54.96 (55.30), H 4.74 (4.47), N 4.33 (4.61), S 10.79 (10.54). UV-Vis (CH₂Cl₂): λ nm (ϵ , M⁻¹cm⁻¹) 268 (5920), 302 (4650),

320 (4210), 440 (620). FT-IR (KBr, cm^{-1}): (ν C-H) 3062, 2959; (ν C=O) 1587; (ν C=C) 1588; (ν C=S) 1259; (γ C=S) 747; (ν Ru-Cl) 283. NMR ^1H 400 MHz, dmso-d₆: δ 7.40 (m, 13H, H4-H6, H7-H11, H7'-H11'), 5.81 (d, 1H, Ar-*p*-cym, $J = 6.2$ Hz), 5.65 (d, 1H, Ar-*p*-cym, $J^3 = 6.2$ Hz), 5.46 (d, 1H, Ar-*p*-cym, $J^3 = 6.2$ Hz), 5.10 (d, 1H, Ar-*p*-cym, $J^3 = 6.2$ Hz), 2.82 (hept, 1H, CH(CH₃)₂), 2.12 (s, 3H, CH₃), 1.18 (m, 6H, CH(CH₃)₂). NMR $^{13}\text{C}\{\text{H}\}$ dmso-d₆ (assignment, δ): C6 181.24, C1 167.26, C2 145.28, C5 145.02, C7 134.62, C7' 134.53, C8 133.19, C8' 132.87, C12 132.27, C12' 132.10, C9-C9' 130.94, C10-10' 129.88, C11-11' 128.79, C8-8' 128.21, C9-9' 126.06, C10-10' 119.60, C11-11' 116.67, CH-C 106.35, CH₃-C 100.06, Ar-*p*-cym 86.35, Ar-*p*-cym 85.49, CH-(CH₃)₂ 29.96, CH-(CH₃)₂ 21.49, .H3 17.86. High resolution ESI(+)MS (acetone): 573.0085[M-Cl]⁺.

Ru(η^6 -*p*-cymene)(L₈)Cl (8). Yellow solid, yield 95 %. MW: 636.06. Elemental analysis for C₃₀H₃₁CIN₂OS₂Ru: C 56.86 (56.63), H 4.63 (4.91), N 4.46 (4.40), S 9.84 (10.08). UV-Vis (CH₂Cl₂): λ nm (ϵ , M⁻¹cm⁻¹) 260 (6820), 314 (6730), 366 (1070), 440 (390). FT-IR (KBr, cm^{-1}): (ν C-H) 3046, 2949; (ν C=O) 1526; (ν C=C) 1526; (ν C=S) 1213; (γ C=S) 744; (ν Ru-Cl) 273. NMR ^1H 400 MHz, dmso-d₆: δ 7.30 (m, 13H, H4-H6, H8-H12, H8'-H12'), 5.70 (d, 1H, Ar-*p*-cym, $J^3 = 6.0$ Hz), 5.64 (d, 1H, Ar-*p*-cym, $J^3 = 6.0$ Hz), 5.56 (d, 1H, Ar-*p*-cym, $J^3 = 6.0$ Hz), 5.41 (d, 1H, Ar-*p*-cym, $J^3 = 6.0$ Hz), 5.18 (m, 2H, H7, H7'), 4.86:4.60 (m, 2H, H7, H7'), 2.75 (hept, 1H, CH(CH₃)₂), 2.12 (s, 3H, CH₃), 1.22 (m, 6H, CH(CH₃)₂). NMR $^{13}\text{C}\{\text{H}\}$ dmso-d₆ (assignment, δ): C6 178.96, C1 166.41, C2 142.94, C8-8' 136.56, C4,C5 136.27, C9-C13 131.94, C9'-C13' 131.07, CH-C 128.79, CH₃-C 128.73, Ar-*p*-cym 128.63, Ar-*p*-cym 128.55, C7 128.35, C7' 127.98, CH-(CH₃)₂ 30.29, CH-(CH₃)₂ 22.01, CH₃ 17.62. High resolution ESI(+)MS (acetone): 601.0688 [M-Cl]⁺.

Interaction with HSA

The experiments were carried out in triplicate and analyzed using the classical Stern–Volmer equation:

$$F_0/F = 1 + K_q \tau_o [Q] = 1 + K_{sv} [Q] \quad (1)$$

where F_0 and F are the fluorescence intensities in the absence and presence of quencher, respectively, $[Q]$ is the quencher concentration, and K_{sv} Stern–Volmer the quenching constant, which can be written as:

$$K_q = K_{sv}/\tau_o \quad (2)$$

where K_q is the biomolecular quenching rate constant and τ_o is the average lifetime of the fluorophore in the absence of the quencher. The binding constant (K_b) and number of complexes bound to HSA (n) were determined by plotting the double log graph of the fluorescence data using:

$$\log [(F_0 - F)/F] = \log K_b + n \log [Q] \quad (3)$$

The thermodynamic parameters were calculated from equation:

$$\ln (K_2/K_1) = [(1/T_1) - (1/T_2)] \Delta H/R \quad (4)$$

where K_1 and K_2 are the binding constants at temperatures T_1 and T_2 , respectively, and R is the gas constant. Furthermore, the change in free energy (ΔG) and entropy (ΔS) were calculated from the following equation:

$$\Delta G = -RT \ln K = \Delta H - T\Delta S \quad (\text{Eq. 5})$$

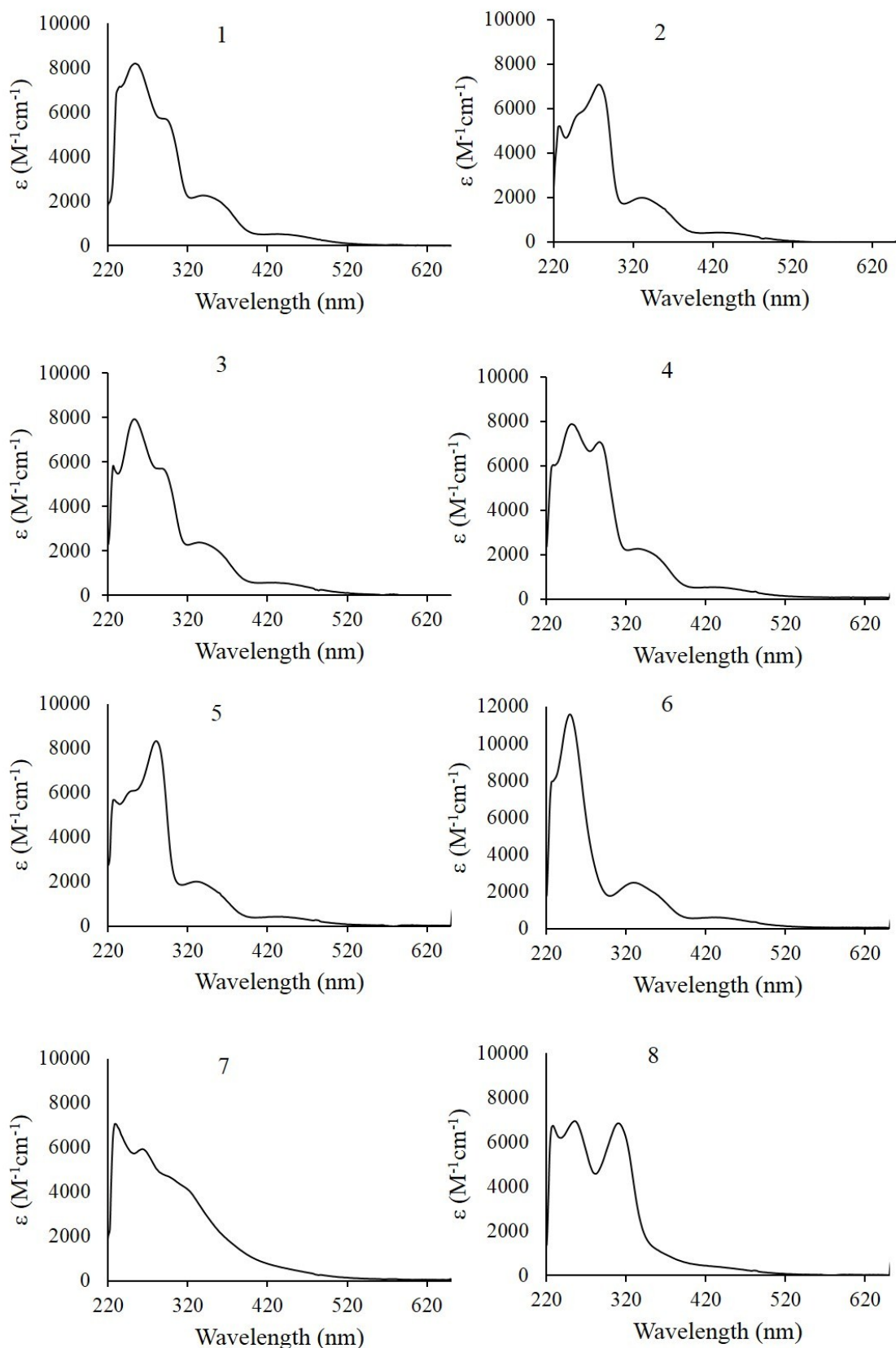


Figure 1S. UV-Vis spectrum of metal complexes in dichloromethane solutions at room temperature

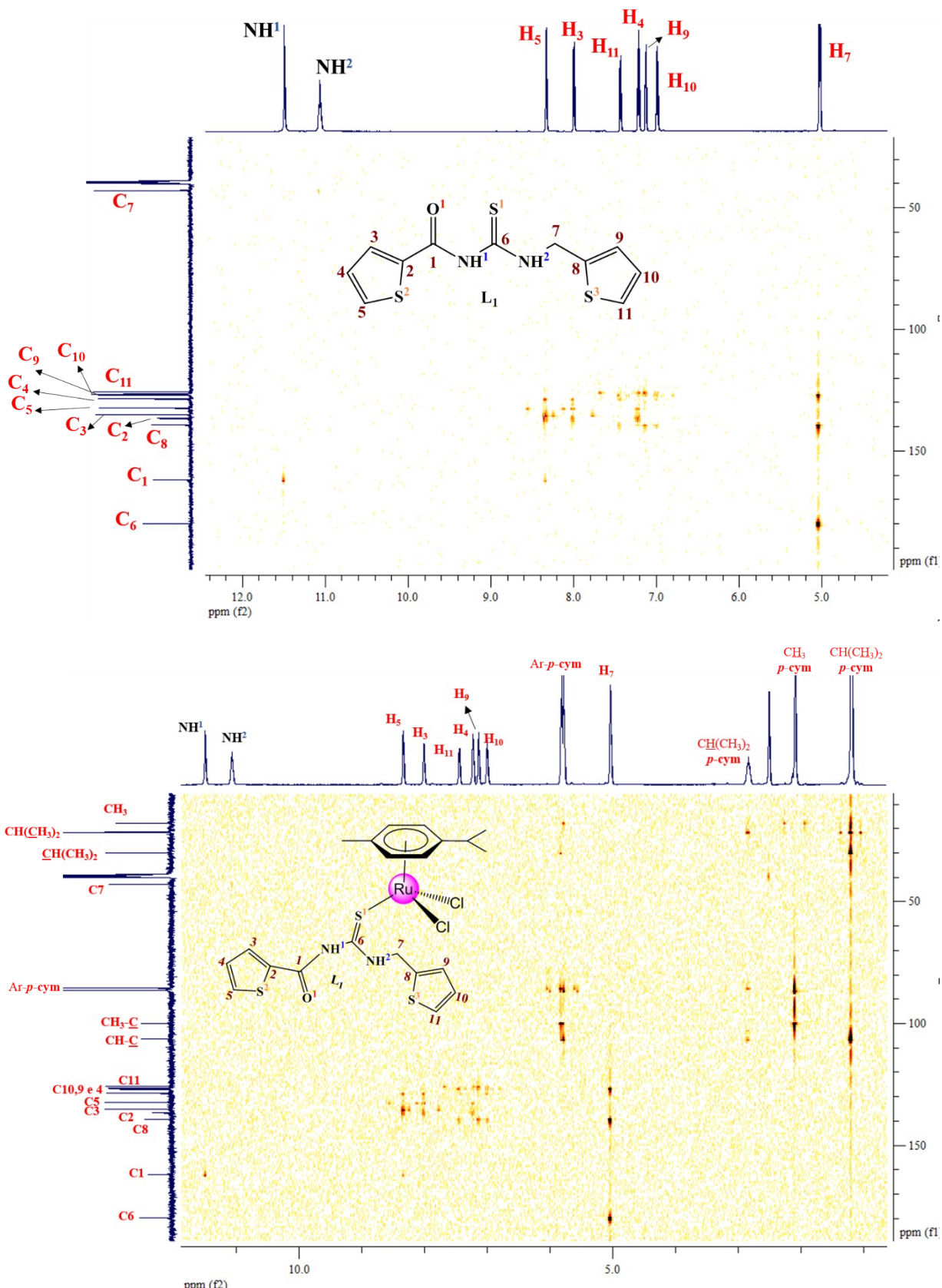


Figure 2S. The 2D heteronuclear ^1H - ^{13}C HMBC NMR spectra of N-thiophenecarbonyl- N' -thiophenemethylthiourea (\mathbf{L}_1) and $\text{Ru}(\eta^6\text{-p-cymene})(\mathbf{L}_1)(\text{Cl})_2$ ($\mathbf{1}$) in DMSO-d_6 at 300 K

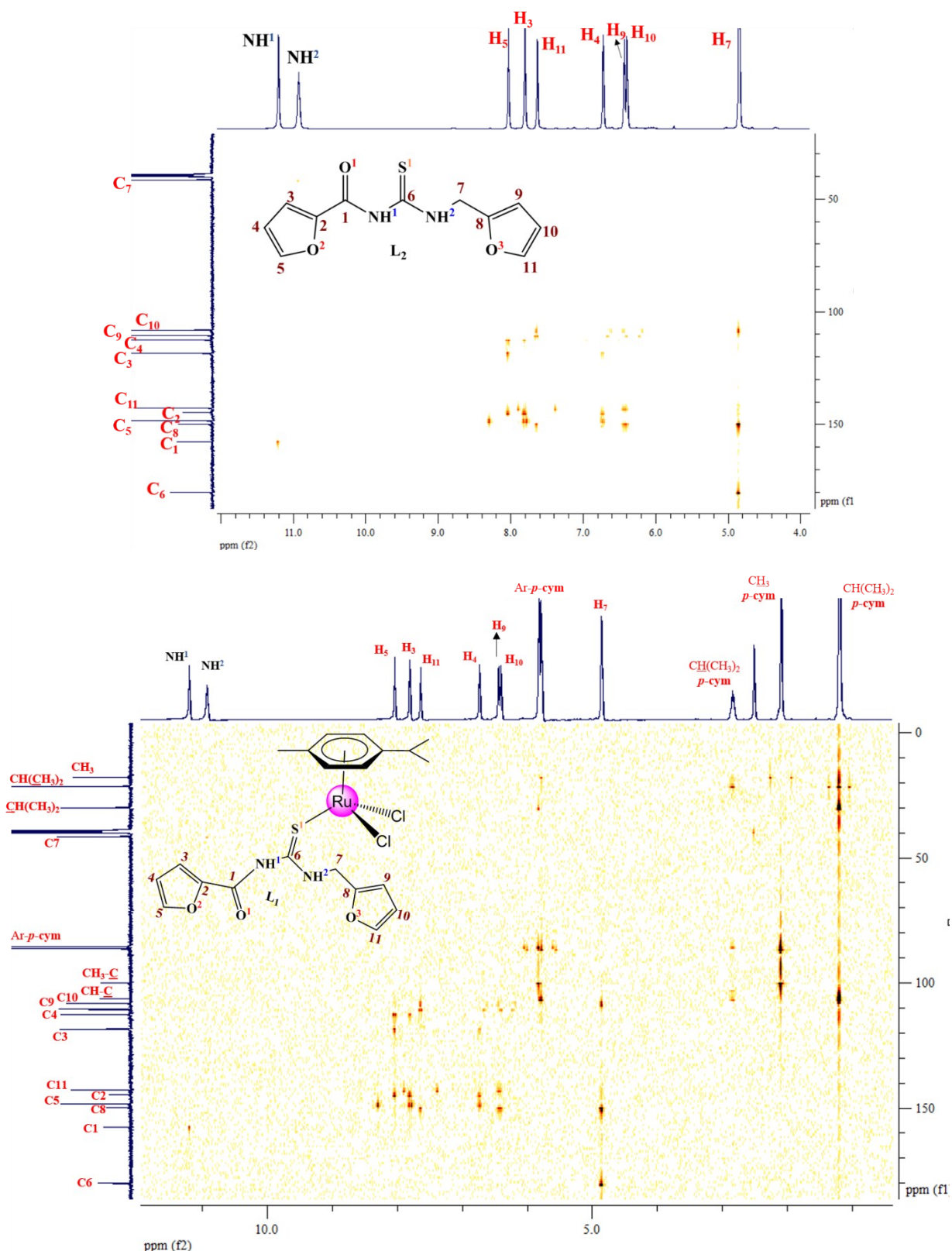


Figure 3S. The 2D heteronuclear ^1H - ^{13}C HMBC NMR spectra of N-furoyl-*N'*-furfurylthiourea (**L₂**) and Ru(η^6 -*p*-cymene)(**L₂**)(Cl)₂ (**2**) in DMSO-d₆ at 300 K

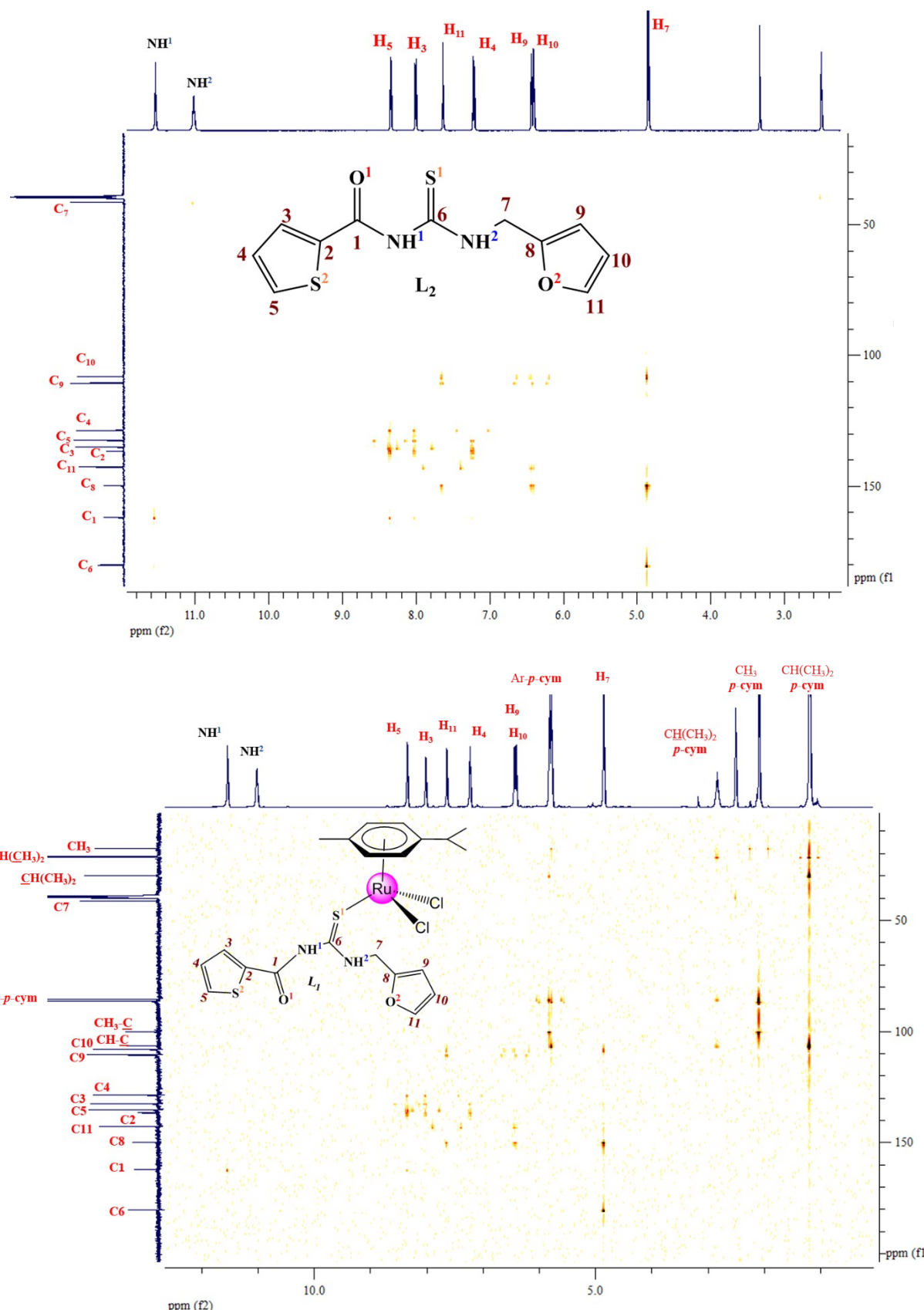


Figure 4S. The 2D heteronuclear ^1H - ^{13}C HMBC NMR spectra of N-thiophenecarbonyl-*N'*-furfurylthiourea (\mathbf{L}_3) and $\text{Ru}(\eta^6\text{-}p\text{-cymene})(\mathbf{L}_3)(\text{Cl})_2$ ($\mathbf{3}$) in DMSO-d_6 at 300 K

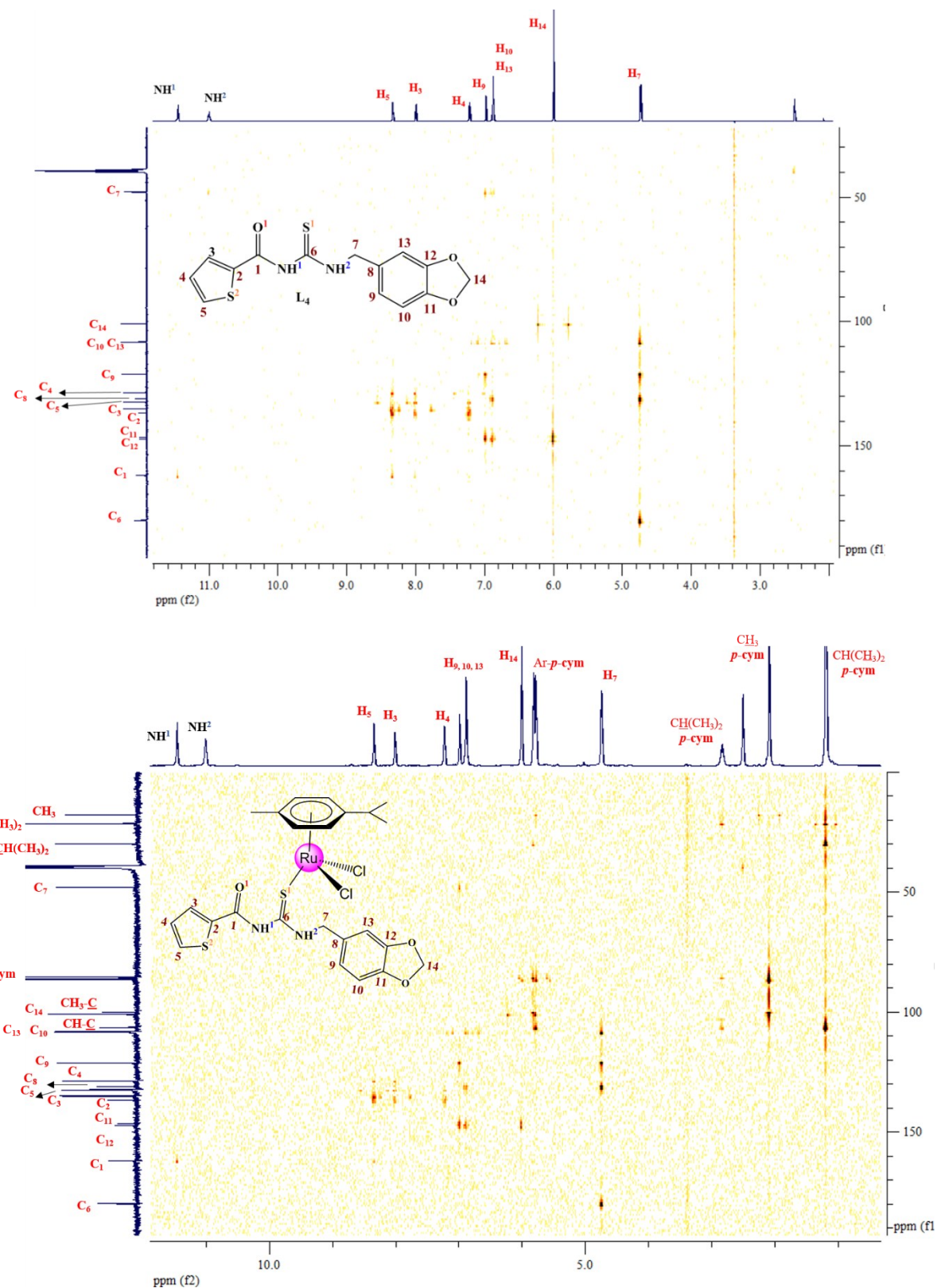


Figure 5S. The 2D heteronuclear ^1H - ^{13}C HMBC NMR spectra of N-thiophenecarbonyl- N' -piperonylthiourea (\mathbf{L}_4) and $\text{Ru}(\eta^6\text{-}p\text{-cymene})(\mathbf{L}_4)\text{Cl}_2$ ($\mathbf{4}$) in DMSO-d_6 at 300 K

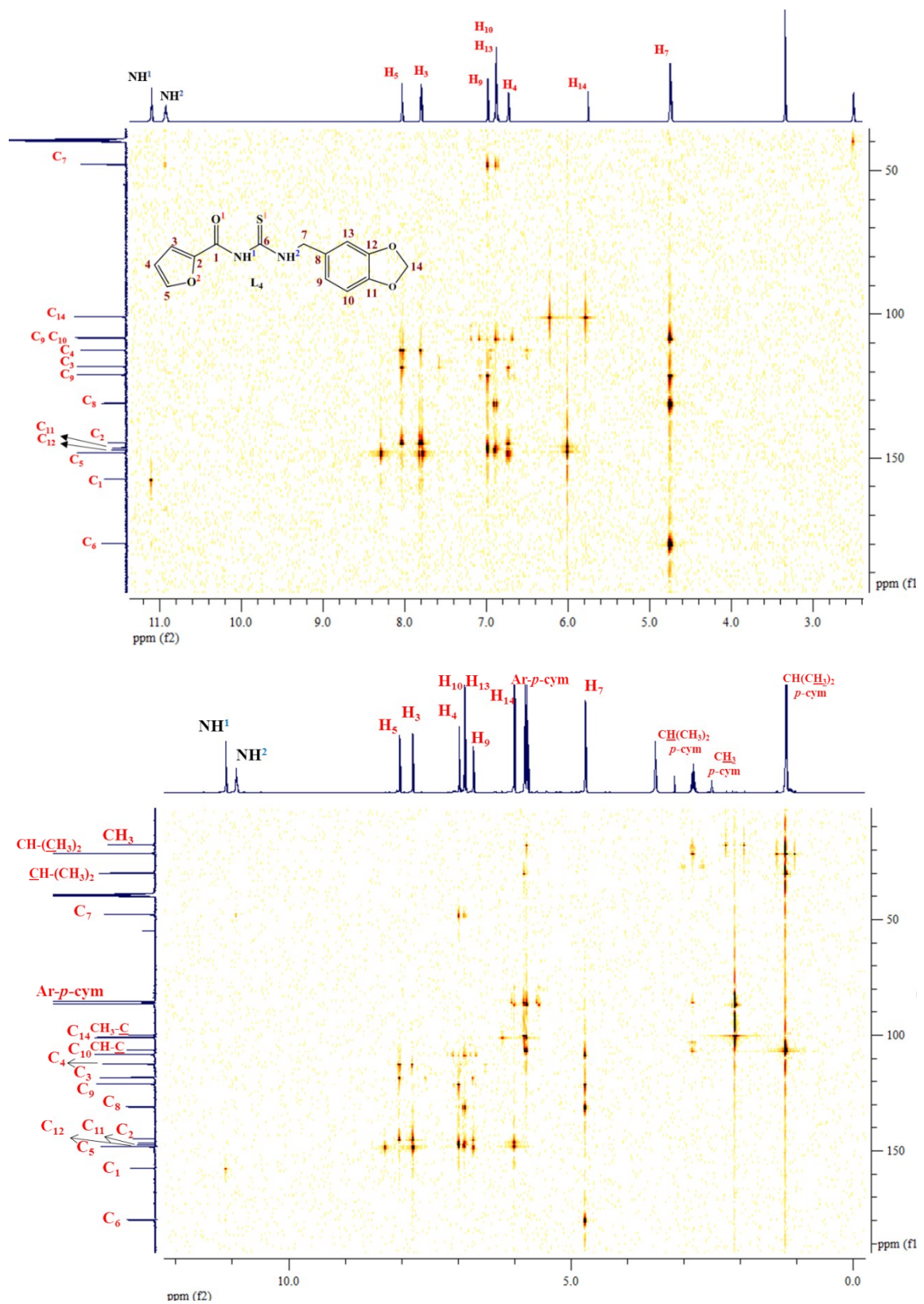


Figure 6S. The 2D heteronuclear ^1H - ^{13}C HMBC NMR spectra of N-thiophenecarbonyl- N' -thiophenemethylthiourea (\mathbf{L}_5) and $\text{Ru}(\eta^6\text{-}p\text{-cymene})(\mathbf{L}_5)(\text{Cl})_2$ ($\mathbf{5}$) in DMSO-d_6 at 300 K

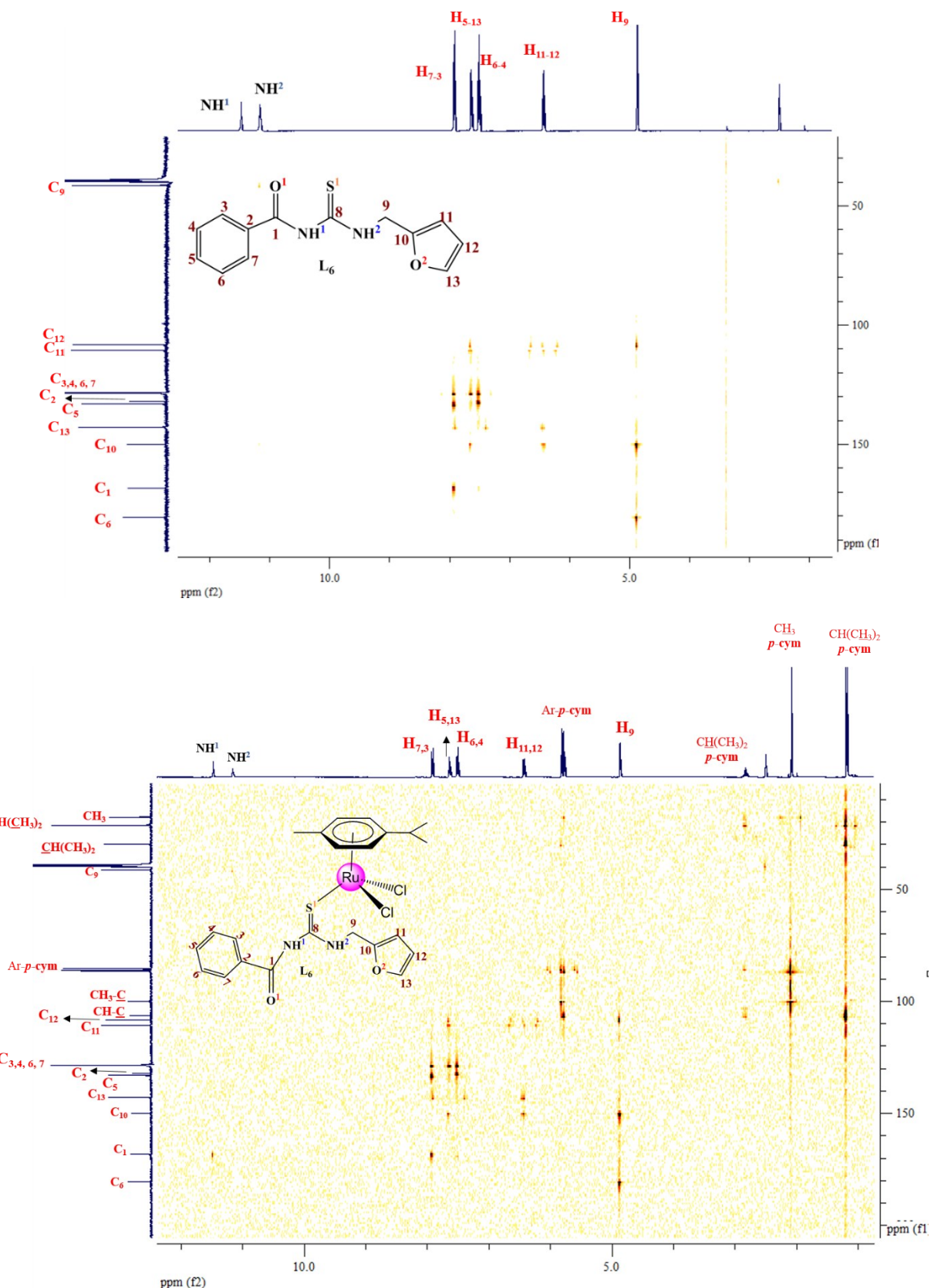


Figure 7S. The 2D heteronuclear ^1H - ^{13}C HMBC NMR spectra of N-thiophenecarbonyl-*N'*-thiophenemethylthiourea (\mathbf{L}_6) and $\text{Ru}(\eta^6\text{-}p\text{-cymene})(\mathbf{L}_6)(\text{Cl})_2$ ($\mathbf{6}$) in DMSO-d_6 at 300 K

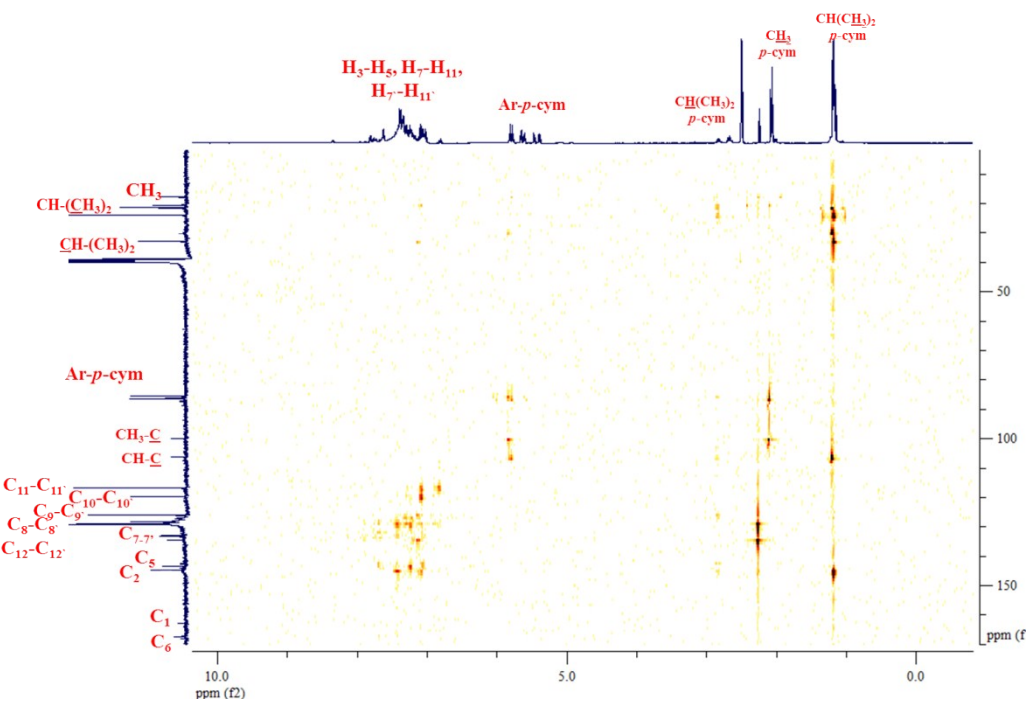


Figure 8S. The 2D heteronuclear ¹H-¹³C HMBC NMR spectra of Ru(η⁶-p-cymene)(L₇)Cl (7) in DMSO-d₆ at 300 K

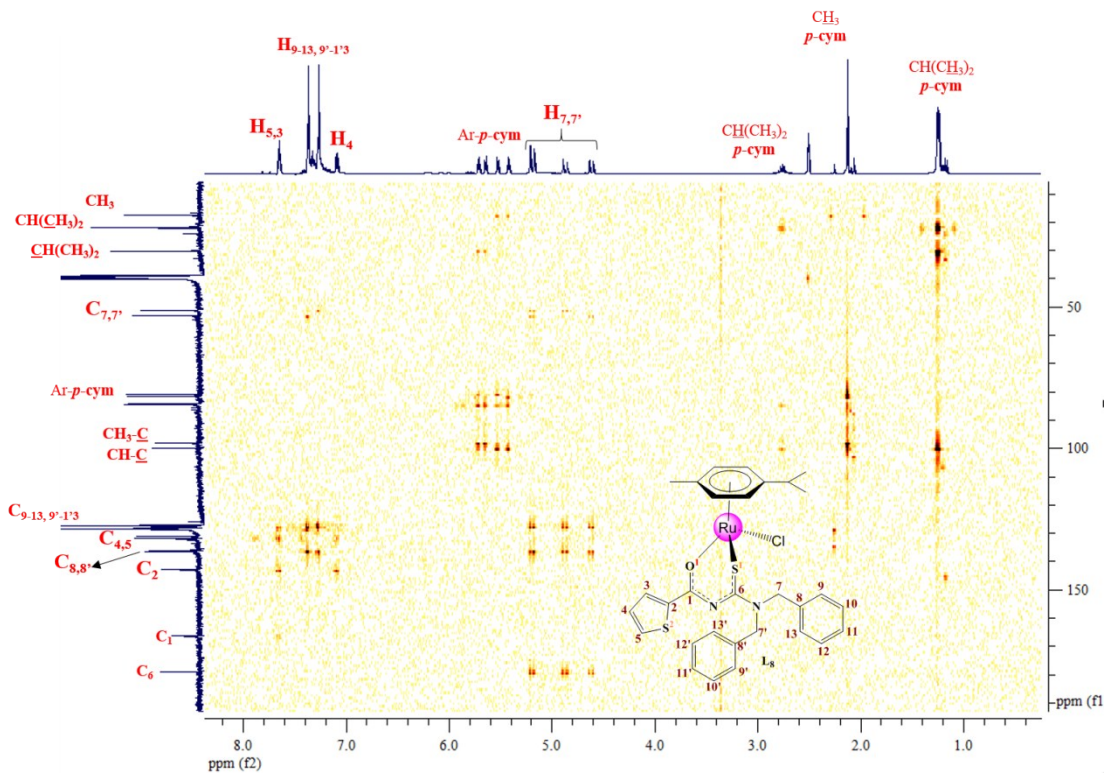


Figure 9S. The 2D heteronuclear ¹H-¹³C HMBC NMR spectra of Ru(η⁶-p-cymene)(L₈)Cl (8) in DMSO-d₆ at 300 K

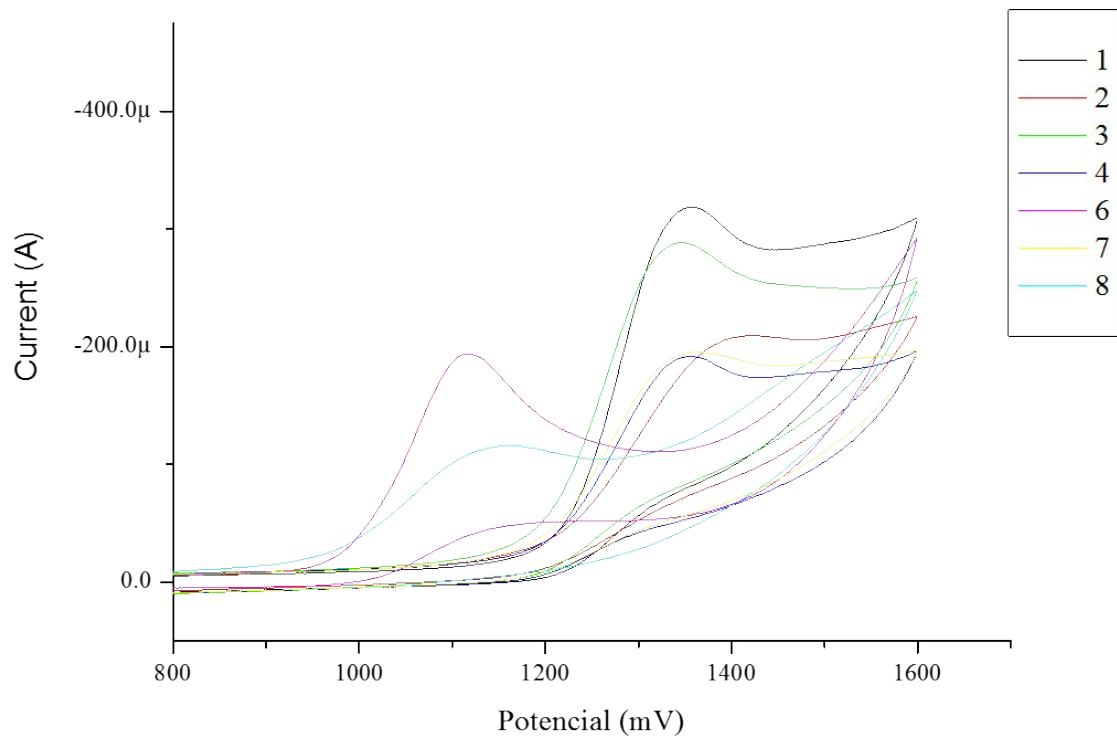


Figure 10S. Cyclic voltammogram for complexes in CH_2Cl_2 , (Tetrabutylammonium perchlorate 0.1 M; Ag/AgCl; work electrode Pt; 100 mV.s^{-1})

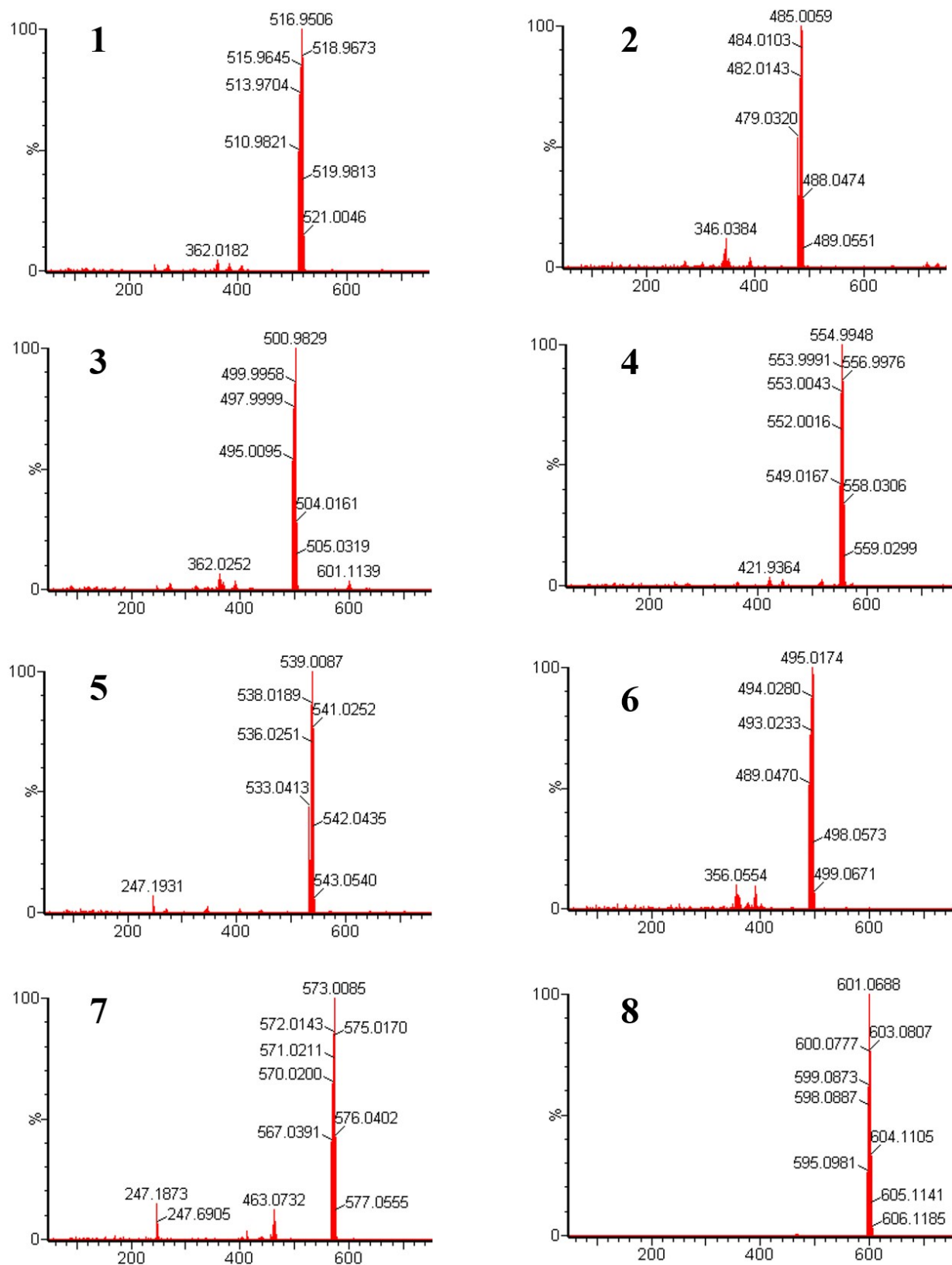
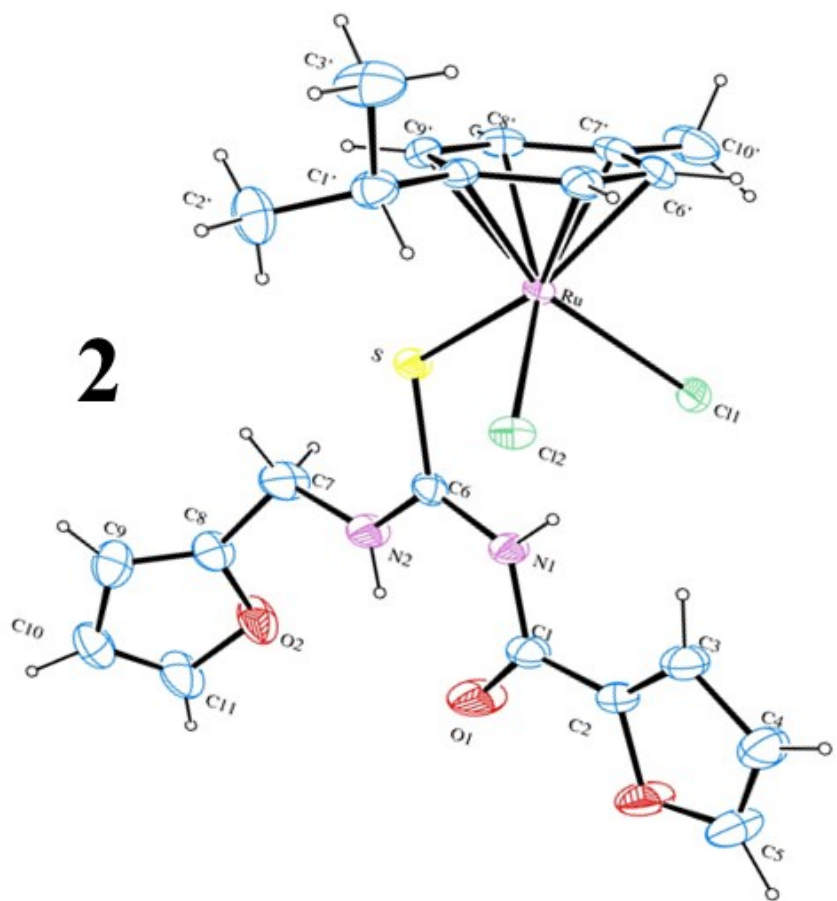
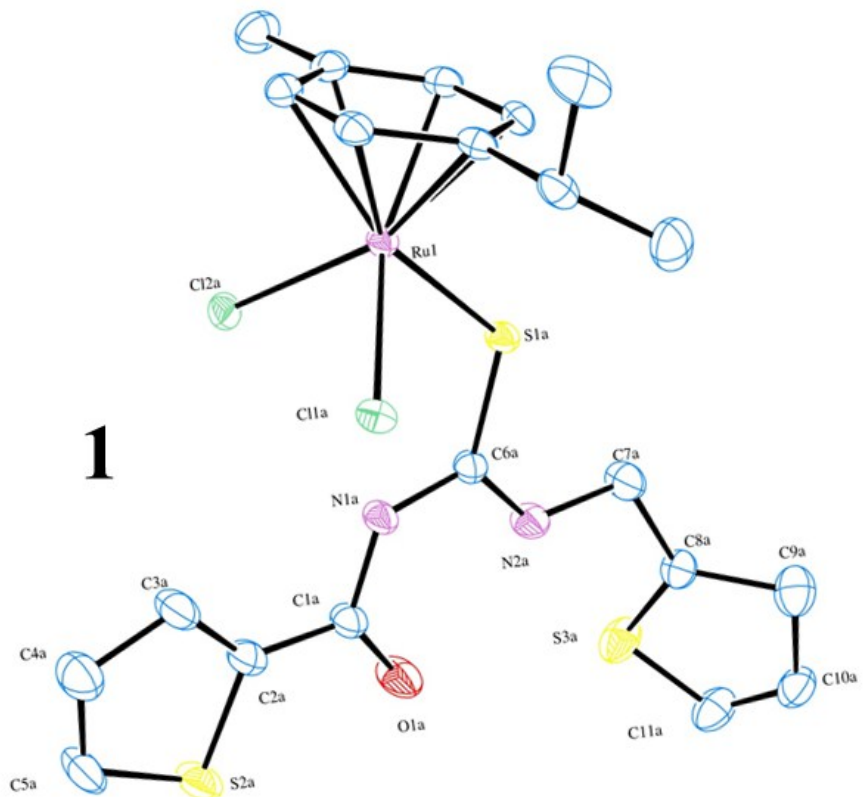


Figure 11S. ESI-MS spectrum of complexes in acetone

Table 1S. Crystal data and structure refinement for metal complexes **1**, **2**, **3** and **6**

Compound	1	2	3	6
Empirical formula	C ₂₁ H ₂₄ Cl ₂ N ₂ ORuS ₃	C ₂₁ H ₂₄ Cl ₂ N ₂ O ₃ RuS	C ₂₁ H ₂₄ Cl ₂ N ₂ O ₂ RuS ₂	C ₂₃ H ₂₅ Cl ₂ N ₂ O ₂ RuS
Formula weight	588.57	556.45	572.51	565.48
Temperature (K)	295(2)	295(2)	295(2)	296(2)
Wavelength (Å)	0.71073	0.71073	0.71073	0.71073
Crystal system	Triclinic	Triclinic	Triclinic	Triclinic
Space group	P1 ⁻	P1 ⁻	P1 ⁻	P1 ⁻
Unit cell dimensions				
a (Å)	10.0900(3)	9.6461(3)	9.6877(3)	9.8652(2)
α (°)	96.796(2)	87.365(2)	86.416(2)	2.8800(10)
b (Å)	15.2550(6)	11.0194(3)	10.9999(4)	10.1852(2)
β (°)	103.806(3)	83.413(2)	82.922(2)	6.4730(10)
c (Å)	16.3192(8)	11.3163(2)	11.4636(4)	12.2154(3)
γ (°)	91.132(2)	76.5380(10)	76.878(2)	77.7850(10)
Volume (Å ³)	2419.19(17)	1161.86(5)	1179.89(7)	1189.57(4)
Z	4	1	2	2
Density (calculated) (Mg/m ³)	1.616	1.591	1.611	1.579
Absorption coefficient (mm ⁻¹)	1.144	1.019	1.088	0.994
F(000)	1192	564	580	574
Crystal size (mm ³)	0.317 x 0.139 x 0.098	0.37 x 0.36 x 0.16	0.494 x 0.312 x 0.087	0.101 x 0.084 x 0.072
Theta range for data collection (°)	2.584 to 25.999	2.600 to 26.000	2.656 to 25.998	1.681 to 25.999
Index ranges	-12 ≤ h ≤ 12, -18 ≤ k ≤ 18, -20 ≤ l ≤ 20	-11 ≤ h ≤ 11, -13 ≤ k ≤ 13, -13 ≤ l ≤ 13	-11 ≤ h ≤ 11, -13 ≤ k ≤ 13, -14 ≤ l ≤ 14	-12 ≤ h ≤ 12, -12 ≤ k ≤ 12, -15 ≤ l ≤ 14
Reflections collected	20500	14110	10251	19305
Independent reflections	9499 [R(int) = 0.0512]	4529 [R(int) = 0.0438]	4585 [R(int) = 0.0668]	4671 [R(int) = 0.1902]
Completeness to theta = 25.242°	99.8 %	99.5 %	99.1 %	100.0 %
Refinement method	Full-matrix least-squares on F ²	Full-matrix least-squares on F ²	Full-matrix least-squares on F ²	Full-matrix least-squares on F ²
Data / restraints / parameters	9499 / 0 / 552	4529 / 0 / 275	4585 / 0 / 275	4671 / 0 / 284
Goodness-of-fit on F ²	1.042	1.182	1.077	1.035
Final R indices [I>2sigma(I)]	R1 = 0.0466, wR2 = 0.1125	R1 = 0.0278, wR2 = 0.0762	R1 = 0.0373, wR2 = 0.0976	R1 = 0.0470, wR2 = 0.1141
R indices (all data)	R1 = 0.0778, wR2 = 0.1341	R1 = 0.0310, wR2 = 0.0797	R1 = 0.0424, wR2 = 0.1023	R1 = 0.0532, wR2 = 0.1177
Extinction coefficient	0.0052(5)	0.0290(18)	0.023(2)	0.0055(13)
Largest diff. peak and hole (e.Å ⁻³)	0.849 and -1.037	0.558 and -0.562	0.815 and -1.167	0.736 and -1.668



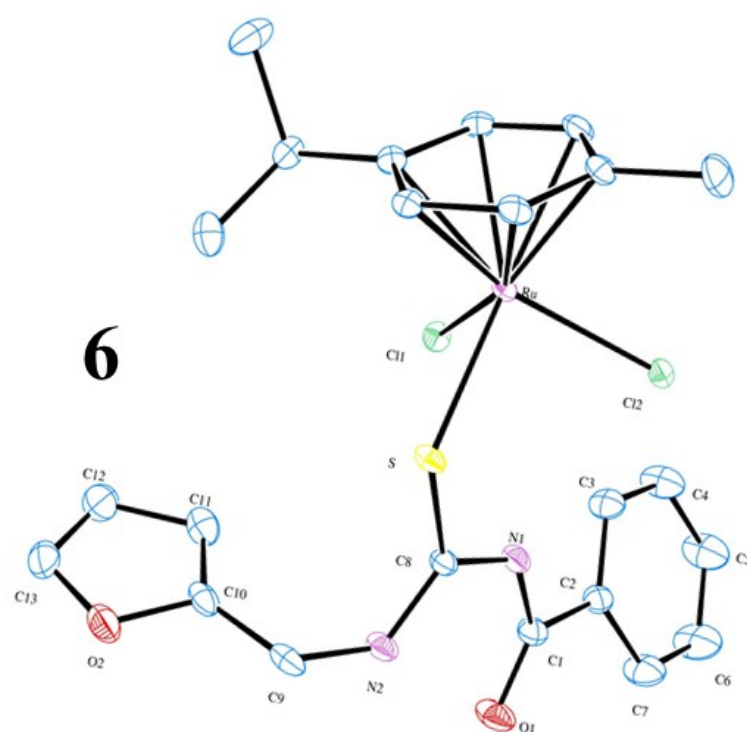
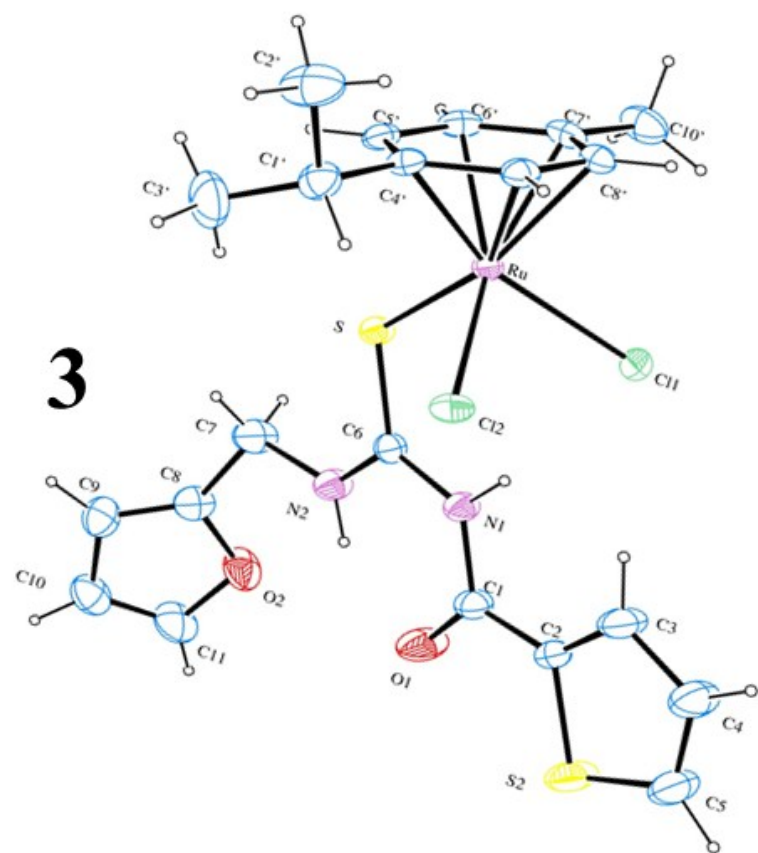
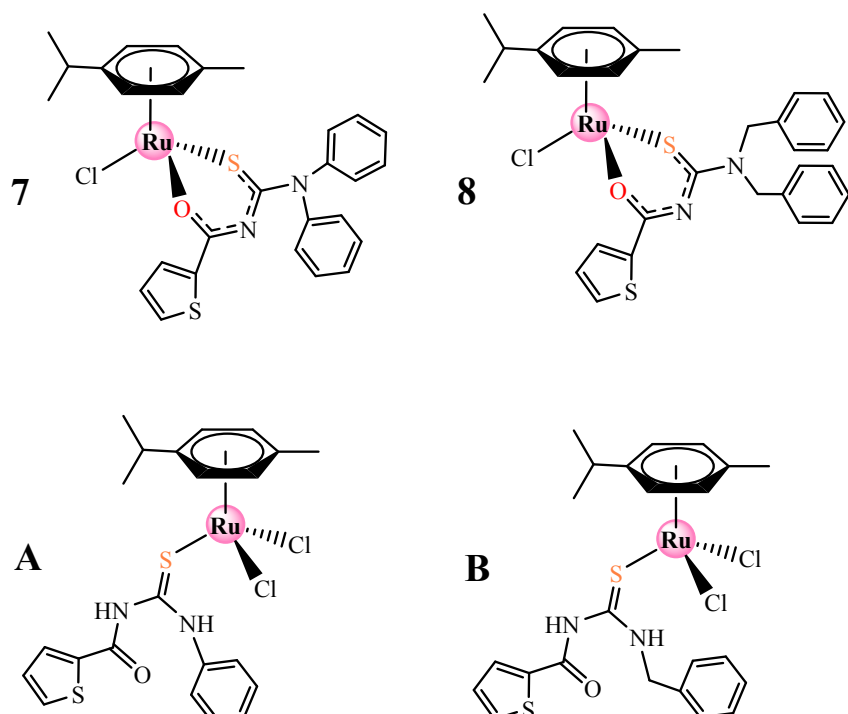


Figure 12S. ORTEP view of complexes **1**, **2**, **3** and **6** with the thermal ellipsoids at the 50 % probability level

Table 2S. IC₅₀ values in 24 h against A549 tumor cell line by MTT assay

Complex	IC ₅₀ (μ M)
7	18.20 \pm 0.85
8	23.10 \pm 0.50
A	90.4*
B	102.1*



*Reference: [Jeyalakshmi, K.; Haribabu, J.; Bhuvaneshb, N. S. P.; Karvembu, R. Half-sandwich RuCl₂(η⁶-p-cymene) core complexes containing sulfur donor aroylthiourea ligands: DNA and protein binding, DNA cleavage and cytotoxic studies. *Dalton Trans.* **2016**, 45, 12518-12531]

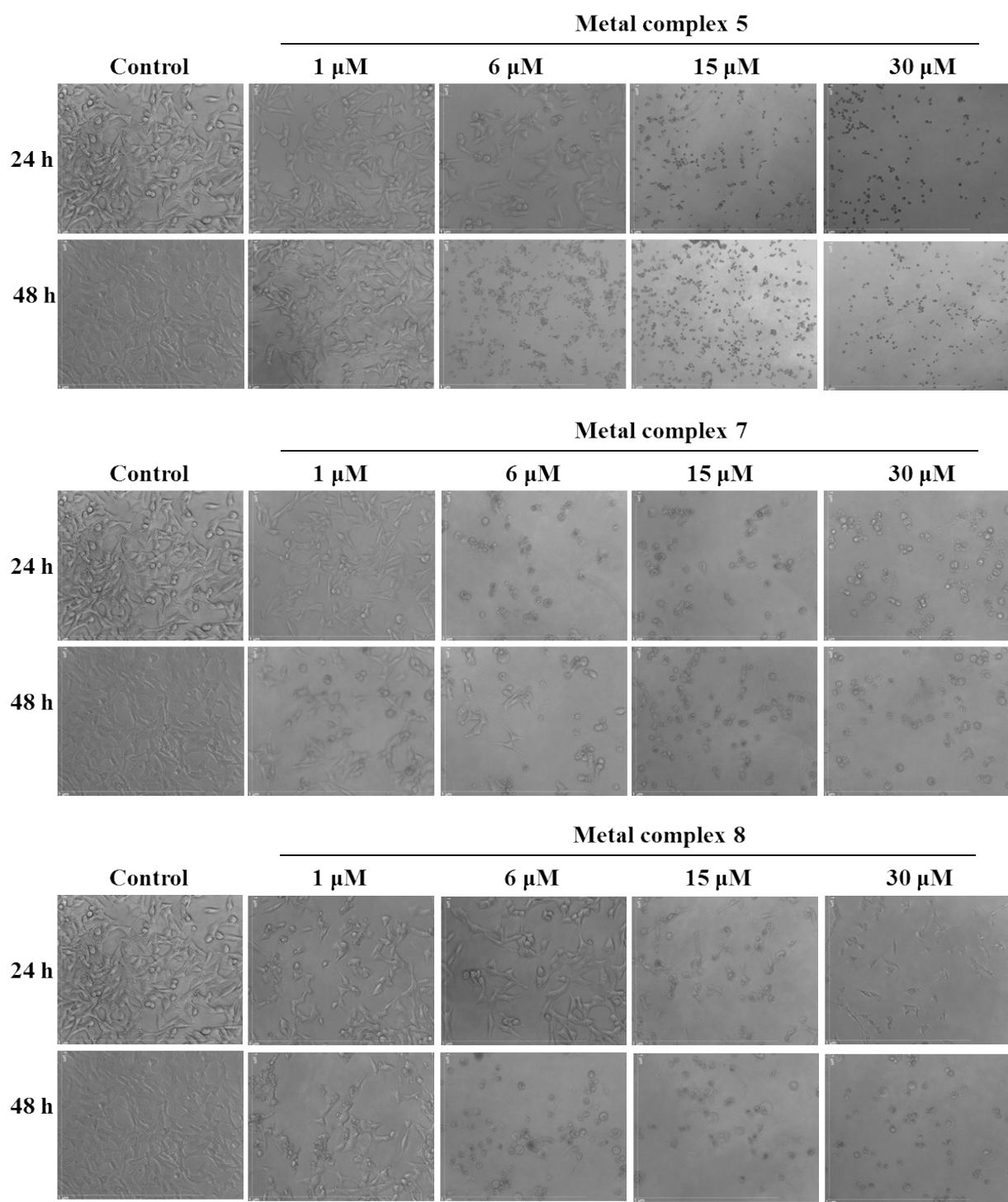


Figure 13S. MDA-MB-231 morphology in different concentrations of Ru-acetylthiourea complexes

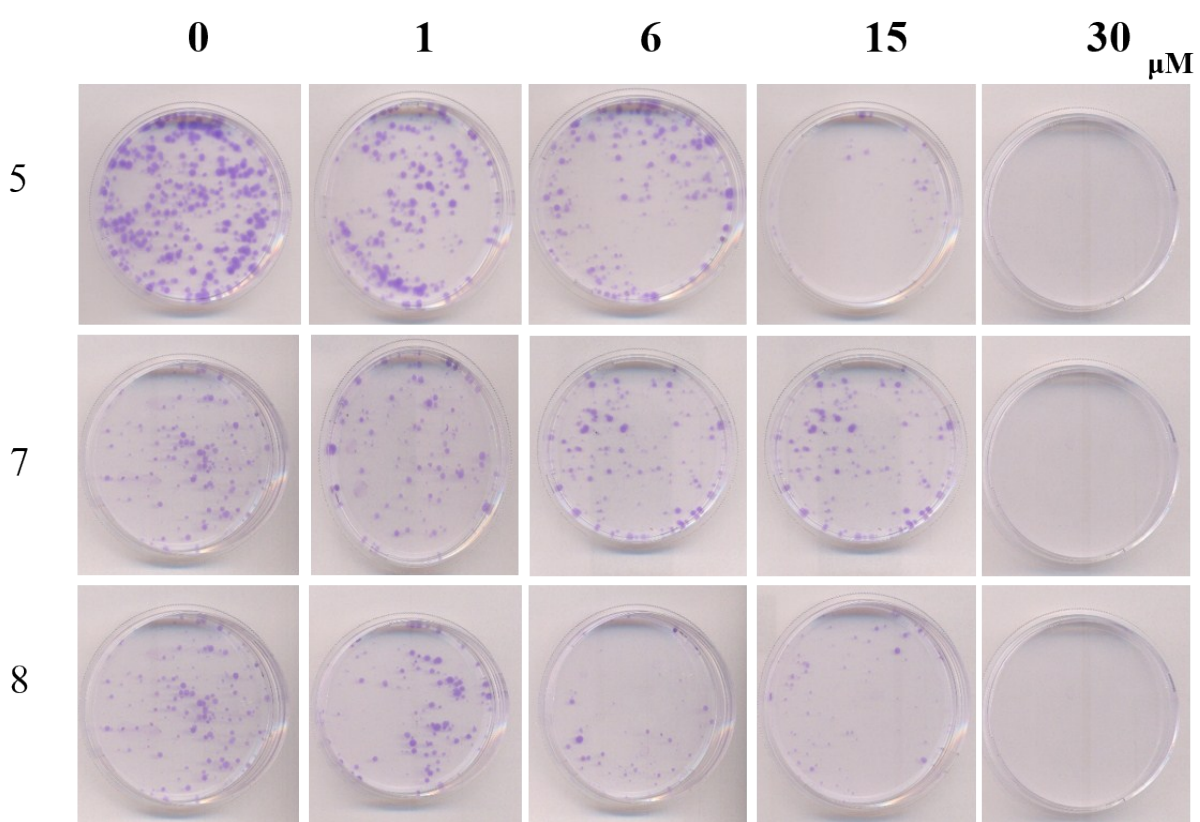


Figure 14S. MDA-MB-231 colony inhibition

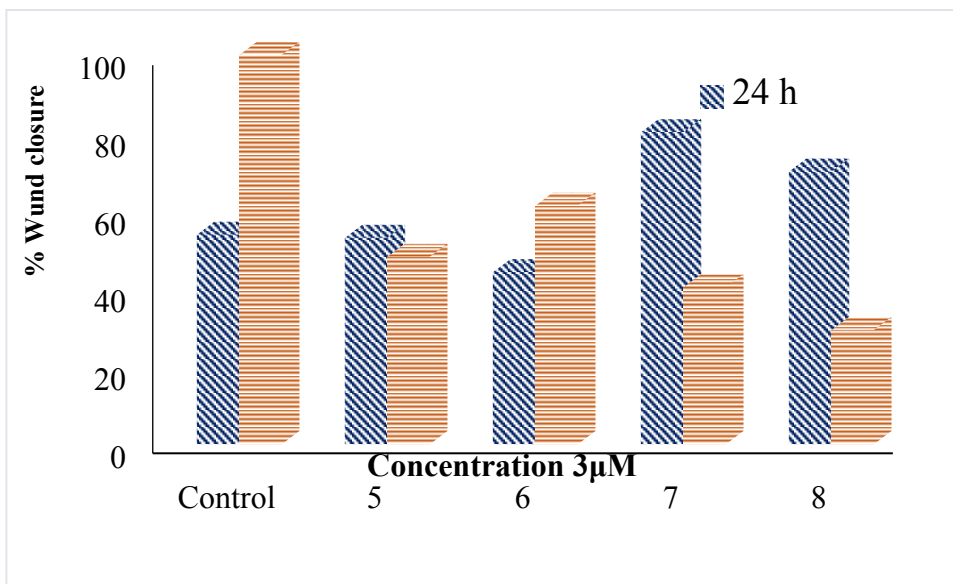
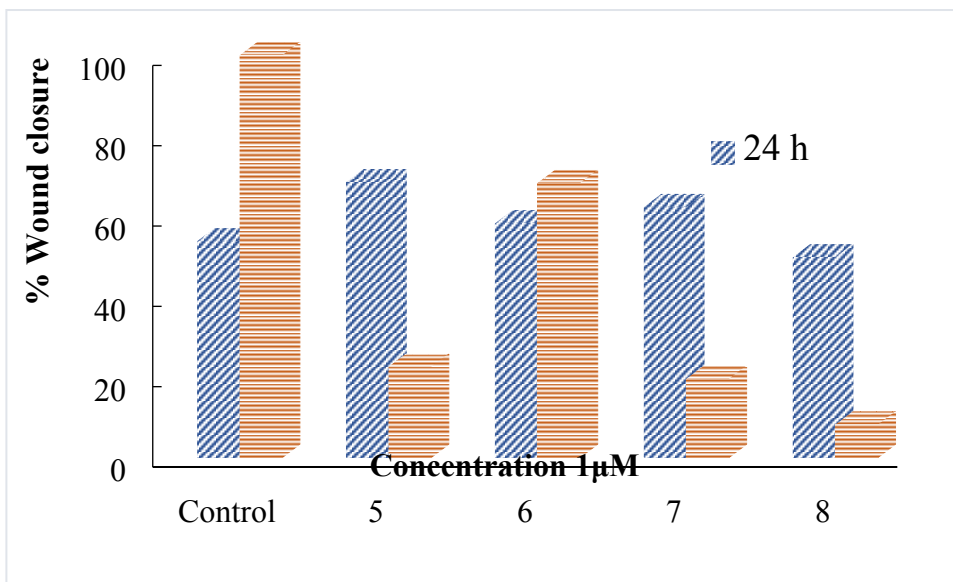


Figure 15S. Wound healing assay

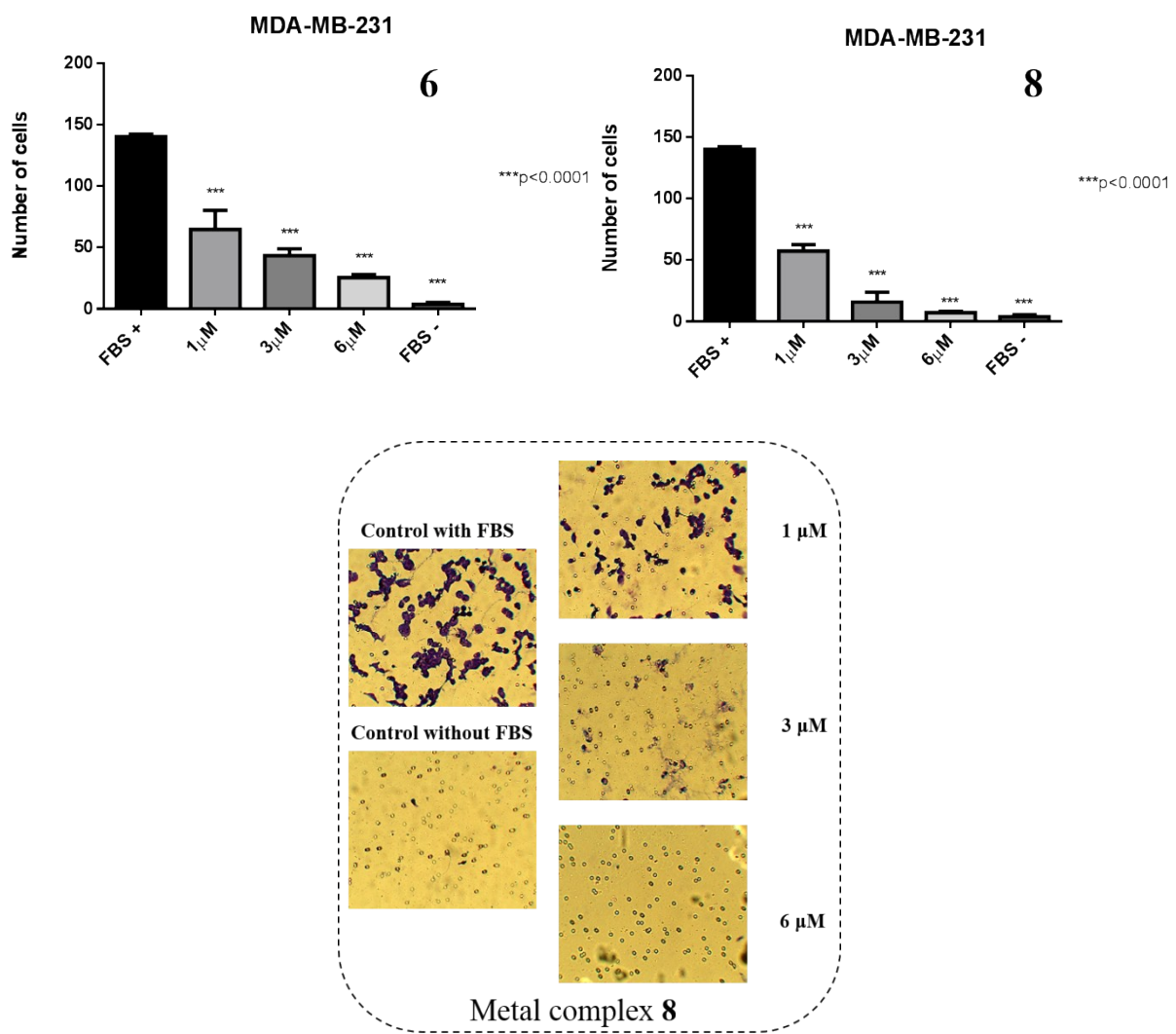


Figure 16S. MDA-MB-231 migration in Boyden chamber assay for metal complexes **(6)** and **(8)**

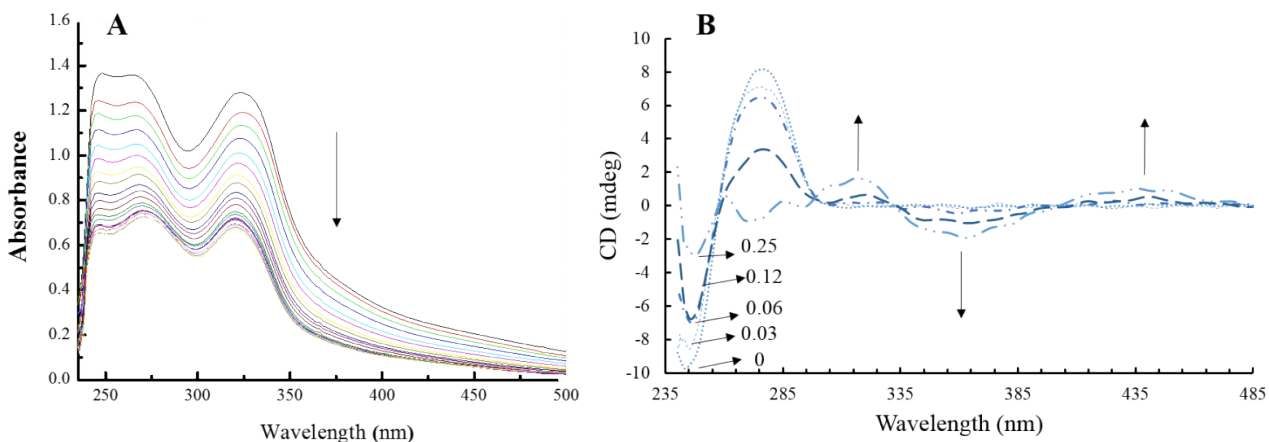


Figure 17S. (A) Spectrophotometric titration spectra of complex **8** calf thymus (CT) DNA. $[DNA] = 0\text{--}1.78 \times 10^{-4}$ M. (B) Circular dichroism (CD) spectra of CT DNA incubated 18 h with the complex **8** at different [complex]/[DNA] ratios at 37°C

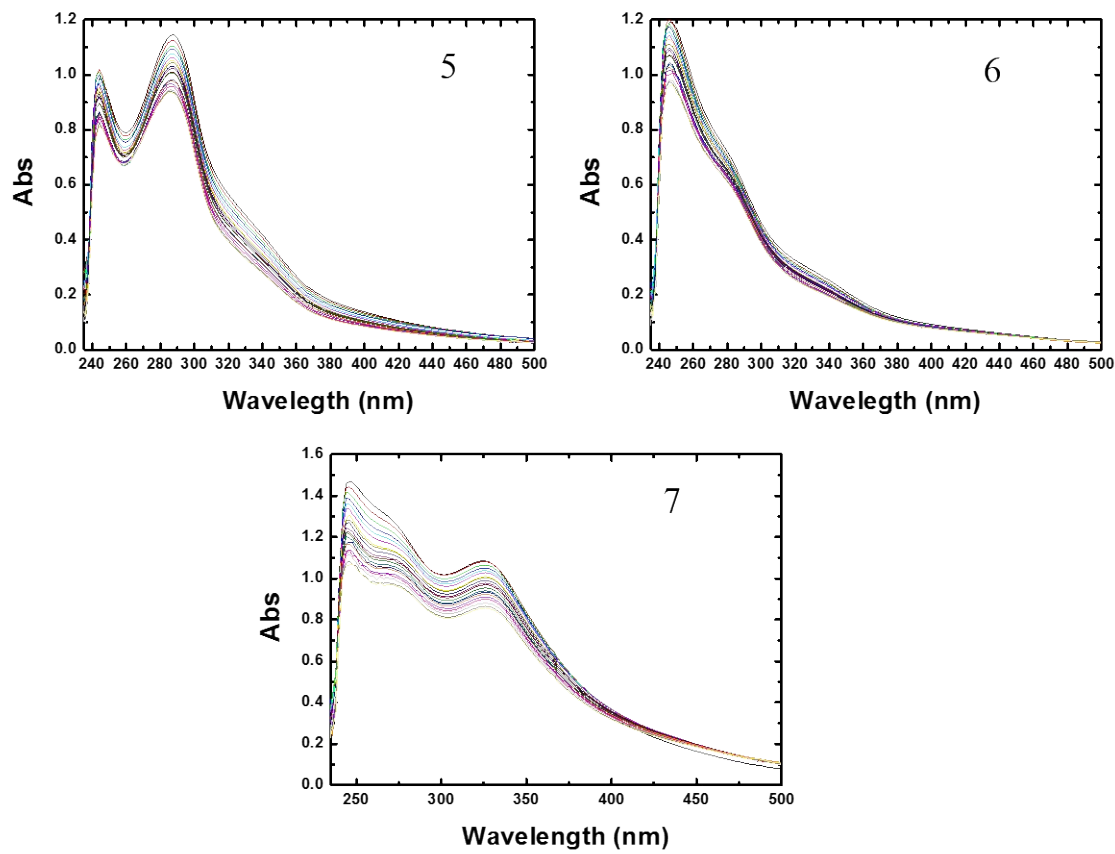


Figure 18S. Spectrophotometric titration spectra of compounds with CT-DNA

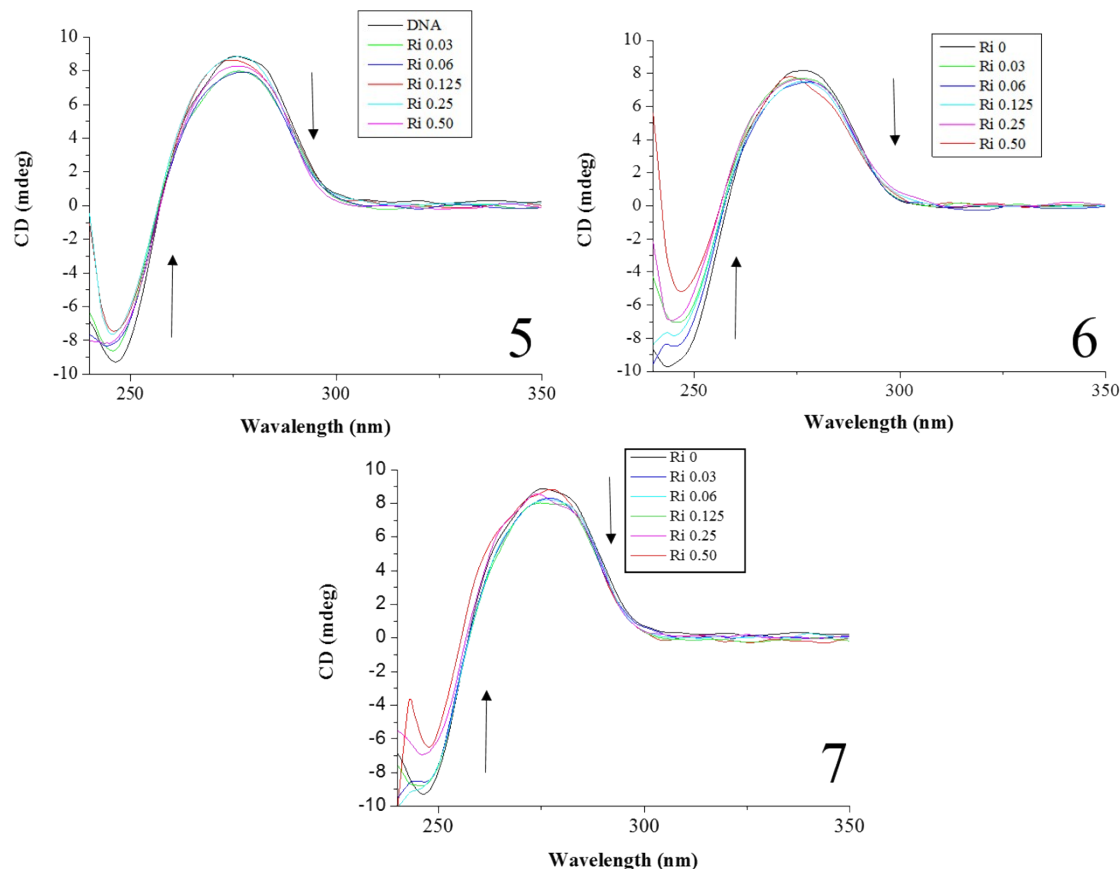


Figure 19S. Circular dichroism (CD) spectra of CT-DNA incubated 18 h with the complexes at 37 °C

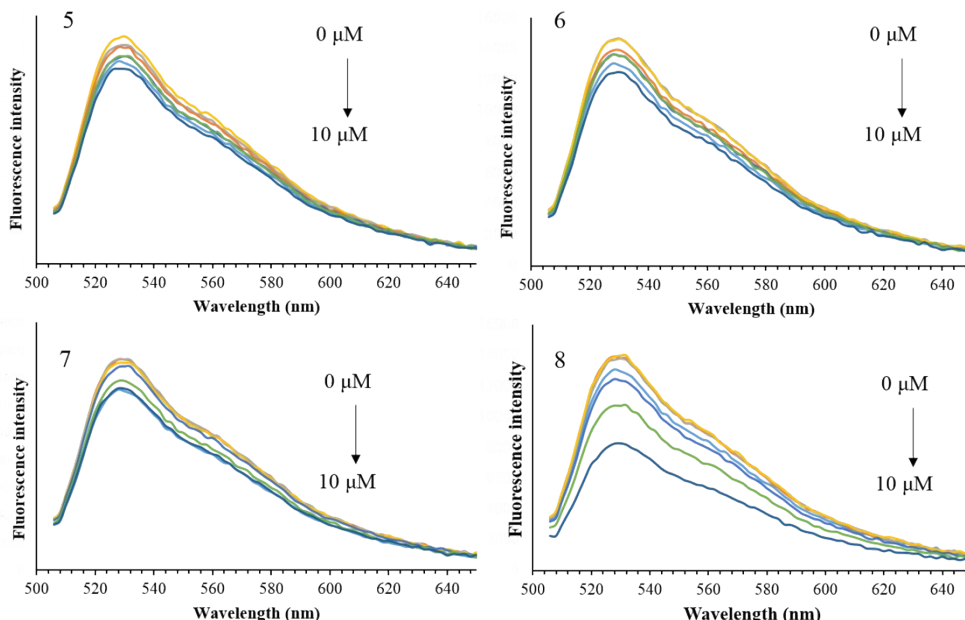


Figure 20S. Effects of the concentration of complexes **5-8** on the fluorescence of DNA-thiazole orange (TO) adduct

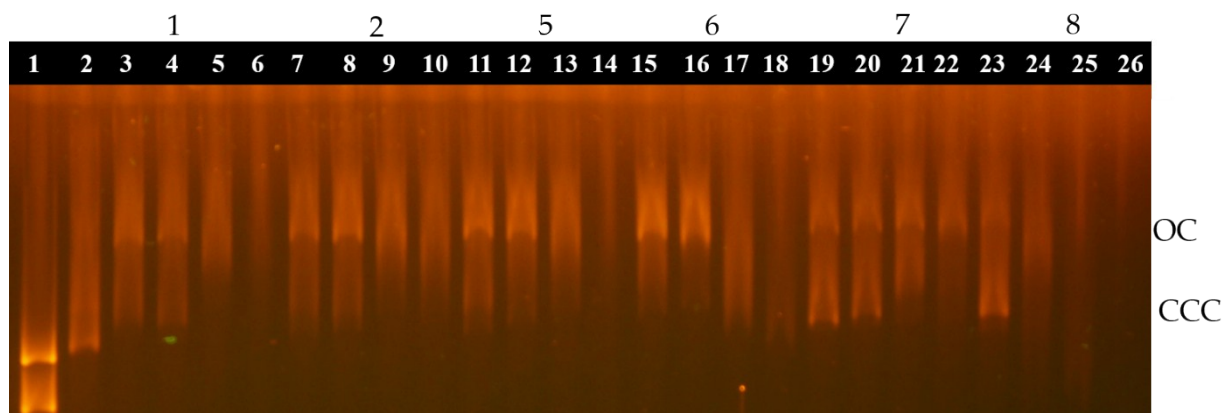


Figure 21S. Effects of the concentration of complexes **1**, **2**, **5-8** on the Electrophoresis of plasmid pBR322 DNA. Molecular weight marker (1) and DNA in DMSO (2). Ri 0.5, 1.0, 2.0 and 4.0 of metal complex **1** (3-6), **2** (7-10), **5** (11-14), **6** (15-18), **7** (19-22), **8** (23-26)

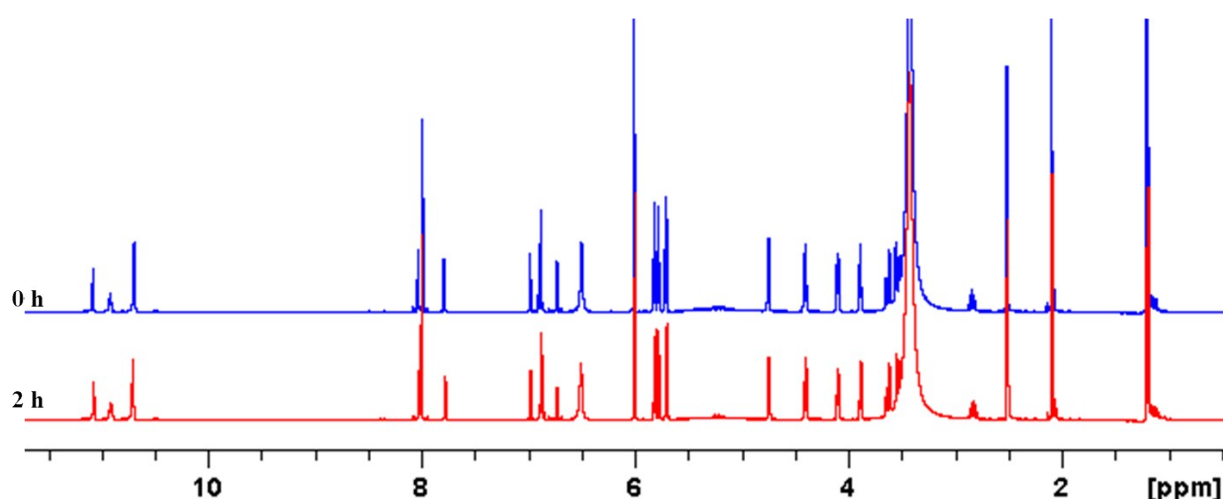


Figure 22S. ^1H -NMR in dmso-d_6 of a mixture of complex **5** and guanosine

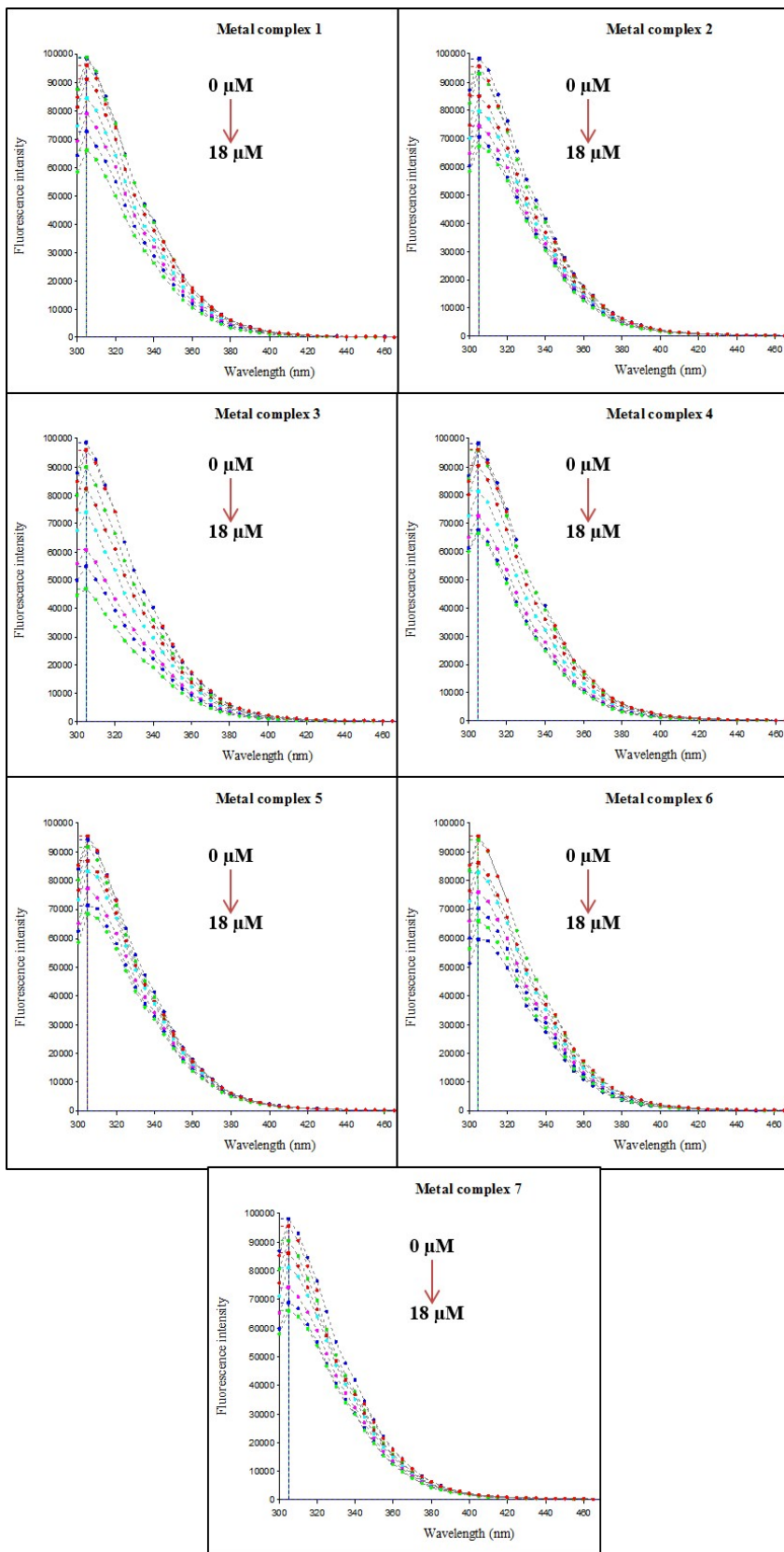


Figure 23S. Fluorescence quenching spectra of HSA with different concentrations of Ru(II)-acylthiourea complexes at 310 K. The arrow shows the intensity changes upon increasing the concentration of the quencher

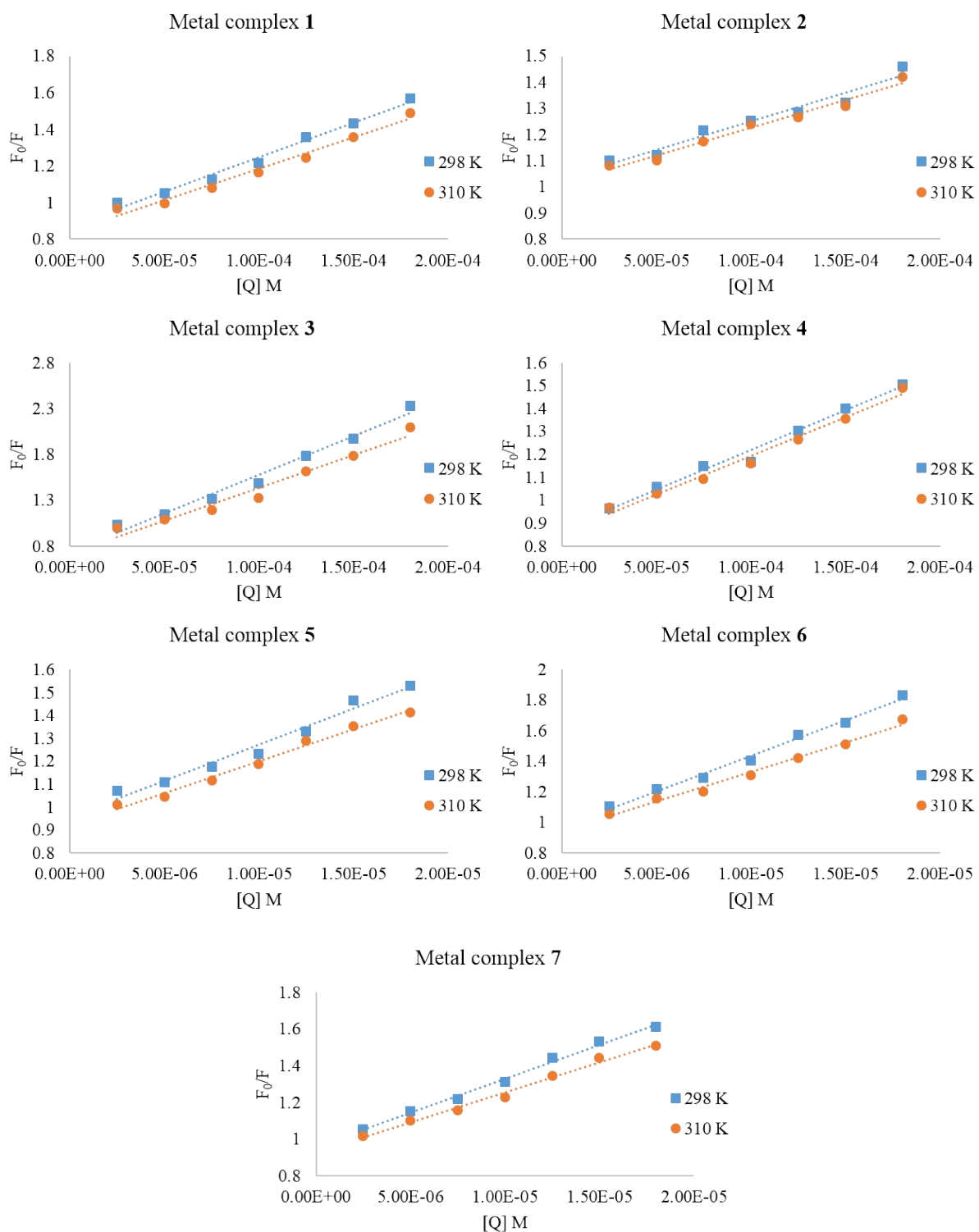


Figure 24S. Stern–Volmer plots showing tryptophan quenching in HSA at different concentrations and temperatures